Fresh-water Fluxes via Pacific and Arctic Outflows across the Canadian Polar Shelf

Humfrey Melling

Fisheries and Oceans Canada, Institute of Ocean Sciences, Box 6000 Sidney BC Canada V8S 3J2

Tom A. Agnew

Environment Canada, Meteorological Service of Canada, 4905 Dufferin St. Downsview ON Canada M3H 5T4

Kelly K. Falkner

College of Ocean and Atmospheric Science, Oregon State University, Corvallis, OR 97331-5503 USA

David A. Greenberg

Fisheries and Oceans Canada, Bedford Institute of Oceanography, Box 1006 Dartmouth NS Canada B2Y 4A2

Craig M. Lee

Applied Physics Laboratory, University of Washington, 1013 NE 40th St. Seattle WA 98105 USA

Andreas Münchow

College of Marine Studies, University of Delaware, 44112 Robinson Hall, Newark DE 19716 USA

Brian Petrie

Fisheries and Oceans Canada, Bedford Institute of Oceanography, Box 1006 Dartmouth NS. Canada B2Y 4A2

Simon J. Prinsenberg

Fisheries and Oceans Canada, Bedford Institute of Oceanography, Box 1006 Dartmouth NS Canada B2Y 4A2

Roger M. Samelson

College of Ocean and Atmospheric Science, Oregon State University, Corvallis OR 97331-5503 USA

Rebecca A. Woodgate

Applied Physics Laboratory, University of Washington, 1013 NE 40th St. Seattle WA 98105 USA

8 Fresh-water Fluxes via Pacific and Arctic Outflows across the Canadian Polar Shelf

8.0 Introduction

Observations have revealed persistent flows of relatively low salinity from the Pacific to the Arctic and from the Arctic to the Atlantic (Melling, 2000). It is customary to associate fluxes of fresh-water with these flows of brine, as follows: the fresh-water flux is the volume of fresh water that must be combined with a volume of reference-salinity water to yield the volume of seawater of the salinity observed. As with sensible heat flux, the choice of reference is arbitrary, but the value 34.8[1] is often used in discussions of the Arctic. This value is an estimate of the mean salinity of the Arctic Ocean (Aagaard and Carmack, 1989) but the data sources and domain of averaging have not been specified. Because the salinity of seawater flowing across the shallow Bering, Chukchi and Canadian Polar shelves is typically lower than 34.8, these flows transport fresh-water from the Pacific to the Atlantic Ocean.

The transfer of waters from the Pacific to the Atlantic has been attributed to the higher sea level of the Pacific (Stigebrandt, 1984; Wijffels, 1992), which is in turn the steric manifestation of lower salinity in the North Pacific relative to the North Atlantic. Calculations referenced to the 1100 dbar level suggest that Atlantic sea level is about 0.65 m lower than the Pacific and 0.15 m lower than the Arctic.

Until recently, the magnitude and variability of these fluxes were poorly known (Melling, 2000). The earliest geostrophic calculations of volume fluxes, based on bottle casts in the 1960s, were still frequently cited. Volume flux had not been measured with established accuracy in any channel. The few existing estimates of fresh-water flux were inadequate, being products of long-term averages (volume flux and fresh-water anomaly) rather than averages of products. The wide variation (32-34: Aagaard and Carmack, 1989; Prinsenberg and Bennett, 1987; Sadler, 1976) in the assumed salinity of through-flow for these estimates is indicative of their large uncertainty, equivalent to a factor of 3 in fresh-water flux. Geostrophic calculations were not referenced to measured currents until the 1980s (Prinsenberg and Bennett, 1987, Fissel et al., 1988).

There were good reasons for our inadequate state of knowledge in the late 1990s, as discussed by Melling (2000). One was political, the bisection of Bering Strait by a national jurisdictional boundary. Another was a geographic peculiarity, namely the proximity of the magnetic pole (80°N 105°W) to the Canadian Archipelago, which renders the geomagnetic field unreliable as a direction reference. Others were logistical – remoteness, harsh climate, persistent pack ice – or technical challenges to observation – strong tides, sea ice, icebergs. Some arose from the nature of the flows themselves, such as small scales of motion, re-circulation and appreciable temporal variability over a wide range of periods. Constraints on numerical simulation included computing capacity and deficient bathymetric and hydrographic information.

The primary recommendation of the late 1990s was more observations. At this time new technology was promising enhanced capability. Doppler sonar offered the potential to measure flow at all depths from locations beyond hazard from drifting ice. Developments in microprocessors had opened up possibilities for smart instruments and new low-power electronics promised much longer operating intervals for sub-sea instruments. New all-weather microwave sensors offered higher resolution for ice reconnaissance, and developments in software permitted the automated tracking of pack drift and deformation.

Some technological challenges remained: how to measure current and salinity in the zone of extreme hazard from drifting ice, the upper 30 m of the ocean where much of the fresh-water flux occurs; how to recover moored instruments from remote areas of the Canadian Archipelago that are rarely free of ice; how to build affordable arrays that resolve the baroclinic scale of motion (5 km) across wide channels; how to measure the direction of current in the vicinity of the geomagnetic pole in the Canadian Arctic. Moreover, numerical simulation of circulation in geography of such complexity was in its infancy.

The ultimate objective of ASOF is to understand the Arctic fresh-water budget and its role in the global climate system. An understanding of the forcing and controls on oceanic fresh-water flux from Pacific to

[1] All values of salinity herein are non-dimensional as appropriate in using the Practical Salinity Scale 1978.

Arctic to Atlantic is a prerequisite for successful parameterization and modeling of the Arctic hydrologic cycle in climate models. Consequently, needs for improved theoretical knowledge were identified in relation to:

- Sea-level differences between Pacific, Arctic and Atlantic basins
- Through-flow forcing by inter-basin differences in sea level
- Forcing by wind and atmospheric pressure
- Dynamics of rotating flow through channels of realistic geometry
- Boundary stress at the seafloor and the ice canopy in tidal channels
- Buoyant boundary flow through a network of 'wide' interconnected channels
- Lagrangian aspects of mixing in channels

A unique aspect of Arctic channel flows is their seasonally varying canopy of pack ice. When the pack is comprised of small floes at moderate concentration, its main impact is on the stress exerted by wind on the ocean surface. However, when large thick floes are present at high concentration, they can jam within the channel (Sodhi, 1977; Pritchard et al., 1979). As ice drift continues downstream of the blockage, an arch becomes evident marking the boundary between open water and fast ice. In addition to its obvious effect of stopping ice flux through straits, a fast-ice canopy reduces the oceanic flux by imposing additional drag at the upper boundary of the flow. Ice cover introduces several additional theoretical challenges:

- Dynamics of pack-ice flow through channels of realistic geometry
- Stable ice-arch formation in channels of realistic geometry
- Dynamical interactions between the flows of water and of pack ice in channels

In the context of climate change, it is interesting to compare the mobility of pack ice that populates the three principal exits routes of ice from the Arctic Ocean. Ice within the channels of the Canadian Archipelago is fast for 8-10 months of the year, when it completely blocks ice export from the Arctic. Within Fram Strait, the pack ice is never fast and there is export of fresh-water to the Atlantic as ice year-round. Ice in Nares Strait flickers between these extremes, sometimes providing an export route year-round and in some years blocking ice drift from December through July.

If the Canadian Arctic channels were simply plumbing, Davis Strait would offer the appeal of metering the total through-flow on a single section, despite its greater width (2.5x the total of other gateways) and cross-section (5x the total). However, the vastness of the Bering and Chukchi Seas and of the Canadian polar shelf precludes their simplification to conduits that convey water without modification from the Arctic to the Atlantic. At least three check points are needed to develop a useful understanding the Arctic's role in the global hydrologic cycle: at entry to Arctic and exit from Pacific, at outflow from the Arctic Ocean over the Canadian polar shelf and at exit from the Arctic and entry to Atlantic.

For practical reasons, observations have been focused at constrictions along the pathways joining the North Pacific to the Atlantic through the Arctic. These are circled and labeled on the map in Figure 1. All inflow from the Pacific Ocean passes through Bering Strait, which is actually more of a gate than a strait since its 85-km width exceeds its length; two islands within the strait obstruct about 9 km of the cross-section. Its greatest depth is 60 m, but there is a sill of 45-m depth about 200 km to the southwest. In contrast, the channels of the Canadian Archipelago are much longer than they are wide. The Archipelago occupies slightly less than half of the Canadian polar continental shelf, which at 2.9×10^6 km^2 represents almost a quarter of the Arctic Ocean area (13.2×10^6 km^2). Its many channels have been deepened by glacial action to form network of basins as deep as 600 m, separated by sills. Deep (365-440 m) sills at the western margin of the continental shelf are the first impediment to inflow from the Canada Basin, but the shallowest sills are in the central and southern parts. For flux measurement, there is an optimal set of relatively narrow, shallow straits through which all flow must pass: Bellot Strait, Barrow Strait (east of Peel Sound), Wellington Channel, Cardigan Strait, Hell Gate and Kennedy Channel. Among these, Bellot Strait is probably of little importance because it has such a small cross-section at the sill (less than 24 m deep, 1.9 km wide).

Although the net flux of volume is towards the Atlantic, water is exchanged in both directions between Baffin Bay and the Arctic Ocean. It is modified by mixing, freezing and melting during the months spent over the shelf and may ultimately be re-circulated back to its source. In contrast to Bering Strait, where re-circulation is usually dependent upon temporal reversals in flow direction, that within the Canadian Arctic is implicit in the spatial pattern of the circulation and the strength of tidally forced mixing and entrainment. The important net fluxes of volume and fresh-water must, therefore, be calculated as the differences between the much larger fluxes in opposing directions through adjacent parts of the cross-section.

Melling (2000) proposed a course of action for study of Canadian Arctic through-flow:

The first priority in future work must be the acquisition of volume-flux values for both Bering Strait and the Canadian Archipelago with useful limits of confidence. An improved understanding of the forcing of these flows is also needed. Subsequently, research might progress to the acquisition of observations sufficient to quantify the fresh-water flux through Bering Strait, and its inter-annual variations. At the same time, technological solutions to the problems of measurement in the Canadian Arctic should be sought. New technology could also be used beneath the heavy ice of the East Greenland Current in western Fram Strait.

It should not be forgotten that the ultimate goal of much research into the dynamics of the global climate system is to predict the response to change. The emphasis here has been on the more modest objective of measuring and understanding present conditions. Until this objective is achieved, prediction of the changes in fresh-water fluxes through the North American Arctic that may accompany dramatic change in climate is beyond our reach.

Long-term maintenance of the infrastructure that is needed for detailed measurements of fluxes at all gateways for through-flow is not realistic. A more tractable methodology for an Arctic observing system in this context involves the integration of data from a few points of continued observation with realistic simulations of through-flow by numerical ocean circulation models; the simulations must be driven in the greater part by observations that are already available. Even the present effort to measure Pacific Arctic through-flow is likely too elaborate to fill this need. A proven capability in numerical simulation of Pacific Arctic through-flow is an outcome that would justify a relaxation of observational diligence.

This chapter starts in a logical geographic progression, exploring recent advances in the empirical knowledge of volume and fresh-water through-flows via Bering Strait into the Arctic and via the principal gateways of the Canadian Archipelago that open into Baffin Bay. In order from southwest to northeast these are Lancaster Sound, Cardigan Strait, Hell Gate and Nares Strait. The subsequent sections make some attempt to integrate over common themes – progress in the numerical simulation of Canadian Arctic through-flow, an ice budget for the Canadian polar shelf via satellite tracking of pack-ice features, meteorological forcing of flow through Arctic sea straits with particular emphasis on orographic effects at the mesoscale, the application of trace chemicals in seawater to elucidation of the sources, mixing and transit times of Arctic through-flow. The final geographically oriented section examines Davis Strait, where the western Arctic delivers its freshwater and other impacts to the convective gyre of the Labrador Sea. A closing section takes stock of our progress in the Arctic sub-Arctic Ocean fluxes study and identifies the issues that impede our understanding of fresh-water flows and dynamics in the North American Arctic.

8.1 Pacific Arctic inflow via Bering Strait

Bering Strait is the only gateway between the Pacific and the Arctic Oceans. On an annual average, the flow through the strait is northwards; it is likely a consequence of decreasing sea level from south to north, Pacific to Arctic, although this postulated gradient has yet to be measured. Regional winds, which are southward on average, oppose flow into the Arctic (Coachman and Aagaard, 1966, 1981; Woodgate et al., 2005b). Melling (2000) provides an overview of early studies.

Measurements of seawater flow through the Bering Strait in recent decades indicate that the average annual flux of volume to the Arctic is about 0.8 Sv (Coachman and Aagaard, 1981; Roach et al., 1995; Woodgate et al., 2005b). Higher estimates from earlier times (e.g. 1.2 Sv in the 1950s: Mosby, 1962) likely reflect the greater uncertainty of measurement using the technology and methods then available. The best estimate of the fresh-water flux through Bering Strait, circa 1990, was 1670 km^3/y [52.9 mSv] relative to 34.8 salinity. In

calculating this value for their review of Arctic Ocean fresh-water, Aagaard and Carmack (1989) used Mosby's value for the average volume flux and an assumed annual average salinity of 32.5 (based mainly on hydrographic measurements in summer during the 1960s and 1970s).

Since 1990, almost continuous measurements of temperature, salinity and current and occasionally ice thickness have been made in Bering Strait at as many as three sites (Figure 2; Roach et al., 1995; Woodgate et al., 2005a). Instruments have been positioned near the seabed to avoid damage from ice keels that frequently extend to 20-m depth. Before 2000, hydrographic sections were measured only sporadically and only in summer (Coachman et al., 1975). Since 2000, sections have been completed every year, again only in summer, and snap-shots of flow structure have been measured several times by ship-mounted ADCP. This recent period of increased observation has provided an improved description of the structure of the Bering Strait through-flow (Woodgate and Aagaard, 2005). In particular new data illustrate the importance of the low salinity Alaskan Coastal Current (Paquette and Bourke, 1974; Ahlnäs and Garrison, 1984) to fluxes of heat and fresh-water through Bering Strait.

An upward-looking ADCP has been operated from a mooring beneath the Alaskan Coastal Current since 2002. Woodgate and Aagaard (2005) interpret recent data to conclude that this stream contributes 220-450 km^3/y [7-14 mSv] to the fresh-water flux. Moreover, previously unacknowledged stratification of the water column in mid strait contributes an additional fresh-water flux of perhaps 350 km^3/y [11 mSv]. The contribution from ice flux is poorly known. The total of these contributions is a flux of fresh-water via Bering Strait equal to 2500 ± 300 km^3/y [79±10 mSv]. This inflow is equivalent to three-quarters of the fresh-water inflow to the Arctic Ocean via rivers.

Annual average values conceal strong seasonal cycles in fluxes through Bering Strait. Monthly mean volume flux is typically higher in summer (1.3 Sv in June), when the dominant southward airflow in this region is weakest (Roach et al., 1995; Woodgate et al., 2005a). The flux decreases in winter under the influence of strong north winds and reaches a minimum of about 0.4 Sv in January. The wintertime increase in salinity further decreases the northward flux of fresh-water; the minimum which occurs in January is 100 km^3/month [38 mSv] (Serreze et al., 2006). In summer, a lower near-bottom salinity, the presence of the Alaskan Coastal Current (April-December) and stronger stratification of surface water throughout the Strait (salinity decreases by 0.5-1 from seabed to surface: Woodgate et al., 2005a) act in concert with the stronger northward current to generate a maximum in the monthly mean fresh-water flux in June of 300-400 km^3/month [115-150 mSv).

A model operating at 9-km resolution has been successful in simulating a seasonal cycle although it is weaker and lagged by two months relative to observations: the modelled fresh-water flux reaches a maximum at 220 km^3/month in July-August and a minimum at 80 km^3/month in March-April (Clement et al., 2005). The discrepancy between the model and observations has two causes: the model generates a lower northward volume flux (only 0.65 Sv) and its resolution of the Alaskan Coastal Current is poor. On the other hand, the observational basis for estimates of flux within the Alaskan Coastal Current is also meagre. Prolonged measurements of the flow and stratification of the Alaskan Coastal Current (now viable using new technology) would reduce uncertainty in this component of the Bering Strait through-flow.

The seasonal cycle in the fresh-water flux through Bering Strait is strongly linked to the seasonal cycle in the volume flux because all water in the Strait in summer is fresher than the 34.8 salinity reference. However, other fresh-water sources to the south, for example the Yukon River, make additional contributions in summer. Although the maximum monthly outflow of the Yukon River is only 40 km^3, the total yearly flow of all rivers into the Bering Sea is 300 km^3 (http://nwis.waterdata.usgs.gov/usa/nwis/discharge; Lammers et al., 2001). However, if the Alaskan Coastal Current is to carry 220-450 km^3/y, there must be other sources of fresh-water. The fresh-water influx from the Gulf of Alaska to the Bering Sea (500 km^3/y: Weingartner et al., 2005) is large enough to be a plausible contributor, but the two-month transit to Bering Strait from the Aleutians complicates explanation of seasonal variation.

Variations in both volume flux and in seawater salinity contribute to the inter-annual variation of fresh-water flux (Figure 3: Woodgate et al., 2006). The annual mean salinity at the seabed was highest in 1991 (32.8), but the highest annual mean volume flux occurred in 1994 (1 Sv). Since 1998, when a better observational

array was established, the fresh-water flux has ranged from 2000 km^3/y [63 mSv] in 1998, to 1400 km^3/y [44 mSv] in 2001 and back to 2000 km^3/y in 2004. The 43% increase between 2001 and 2004 equals almost one quarter of the total annual inflow to the Arctic from rivers. Weakened north winds and consequent increased volume flux (0.7 to 1.0 Sv) explains 80% of the increase in fresh-water flux over this period (Woodgate et al., 2006). Clearly atmospheric variability in the Bering-Chukchi region has important influence on the Arctic fresh-water budget.

Note that the fresh-water flux estimates in the preceding paragraph (1400-2000 km^3/y) do not include the fresh-water transported within the Alaskan Coastal Current and the low-salinity surface layer. Investigators now acknowledge that combined fresh-water fluxes via the surface intensified Alaskan Coastal Current and within the low salinity upper layer across the Strait are likely 800-1000 km^3/y [25-32 mSv], or more than one-third of the total. Without measurements of the upper half of the water column across the Strait, our ability to describe inter-annual variation in fresh-water flux is compromised. Existing data suggest that the amplitude of inter-annual variability will increase when such observations become available.

New autonomous instruments (notably IceCAT, an upper-layer sensor in a trawl-resistant housing that transfers data to a recorder at safe depth) may provide the means for year-round measurement in the upper ocean where risk from storm waves and ice-ridge keels is high. Information from sensors on Earth satellites may also play a role. For example, the northward flow of river-freshened seawater in the coastal current is revealed by its higher temperature proxy in thermal-band satellite images (Figure 2). Satellite-borne radar altimeters have also been used to estimate the variability of flux through Bering Strait via direct measurements of sea level and the assumption of geostrophy (Cherniawsky et al., 2005).

International politics have been an impediment to flux measurement in Bering Strait, which is split between the Exclusive Economic Zones of the United States and Russia. Since 2004, a joint US-Russian scientific programme RUSALCA (Russian-American Long-term Census of the Arctic), lead in the USA by NOAA, has facilitated the installation of instruments on moorings in the western channel of the Bering Strait.

8.2 Flux and variability in Lancaster Sound

Lancaster Sound is the southernmost of the three principal constrictions to flow across the Canadian polar shelf between the Arctic Ocean and Baffin Bay. An array of instruments has been in place on moorings in western Lancaster Sound since 1998, with intent to measure the combined outflows of seawater from Barrow Strait to the west and Wellington Channel to the north-west. Lancaster Sound is 68 km wide at this location and has a maximum depth of 285 m (Figure 4). The array has evolved as new technology became available.

The location in Lancaster Sound is ice covered for as long as 10 months every year and typically lies beneath fast ice for half this time. It is well positioned logistically because it can be conveniently serviced in August via icebreakers of the Canadian Coast Guard that routinely operate near Resolute Bay. Moorings have been recovered and redeployed annually and a modest hydrographic survey has been completed via CTD, with water sampling for analysis of geochemical tracers.

Arctic surface water occupies the upper part of the instrumented section. In summer, the coldest water (-1.7ºC, 32.8-33.0 salinity) is a remnant of winter at 50-100 m depth (Prinsenberg and Hamilton, 2005). Above this layer lies less dense surface water formed by addition of ice melt-water and runoff and warmed by insolation. The lightest water is organized into buoyancy boundary currents that flow in opposite directions against the northern and southern shores. Below the remnant winter waters, the temperature and salinity increase with depth. Some of this water has arrived from the north and west (Melling et al., 1984; de Lange Boom et al., 1987) but the warmest and most saline is derived from the West Greenland Current in Baffin Bay to the east.

Because the keels of ice ridges threaten near-surface instruments, moorings have not extended above 30-m depth. For this reason, the array incorporates an ICYCLER in addition to the familiar instruments for measuring current, temperature and salinity. The ICYCLER periodically deploys a buoyant temperature-conductivity module upwards to the ice, measuring fresh-water and heat in the hazardous part of the water column. A comparison has revealed that a fresh-water inventory calculated using ICYCLER data is 20% larger during June to October than that inferred by extrapolation from data recorded by a temperature-

conductivity sensor fixed at 30-m. Since flow speed may also increase towards the surface, the impact of accurate surface date on computed fresh-water flux is even more dramatic. Data from a sensor at 30-m depth are a better measure of the near-surface fresh-water inventory during the cold part of the year in Lancaster Sound, when the surface mixed layer extends below 30 m.

Since 2004, the array has also included ice-profiling sonar (IPS). Pack-ice draft measurements by this instrument in combination with ice tracking data from the ADCP provide the component of fresh-water flux moved by pack-ice (e.g. Melling and Riedel, 1996). Results are not yet available.

Reliance on the magnetic compass for a reference direction is standard practice in oceanography. However in western Lancaster Sound only 800 km from the north magnetic pole, the horizontal component of the Earth's field is less than 2500 nT, the inclination of field lines is almost vertical (87.6°) and the magnetic declination is significantly perturbed by ionospheric effects over a range of time scales. To use a geomagnetic reference under such conditions, instrument orientation must be measured using a precise 3-axis fluxgate compass and the instantaneous geomagnetic vector must be monitored at a nearby geomagnetic observatory. In Lancaster Sound the latter is conveniently located in Resolute Bay. Details are provided by Prinsenberg and Hamilton (2005).

For the section measured in August 1998, geostrophic calculations revealed an eastward current that extended across two-thirds of the Sound but was strongest at the surface near the southern shore (Prinsenberg and Hamilton, 2005). There was weak westward flow at depth on the northern side. Subsequent study has shown that flow through the northern third of the section is quite variable and contributes little to net flux on a long-term average. The existing array of moored instruments provides observations of current, temperature and salinity at only 2-4 positions across the section.

In computing fluxes, we have assumed that data from each location and depth of measurement represent average conditions across a specified sub-area of the cross-section; fluxes are calculated as the sum of area-weighted data. The selection of sub-sectional areas was guided by data from an expanded array of four sites in place during 2001-2004. This array provided the usual observations at sites in the coastal boundary currents near the southern and northern shores, plus observations of near-surface (0-60 m) current at the quarter and half-way points from the southern shore (Figure 4). Figure 5 displays the average of currents measured at 10, 30 and 50 m as weekly averages for three sites at 15-km spacing in the southern half of the section. At times, most often during November through May, upper ocean flow was similar at all three sites. However during the summer the shear across the channel was large; the speed at the southernmost mooring was almost twice the average value for the 3 sites. A seasonally varying weighting of data from the southernmost mooring has therefore been used in calculating fluxes at times when only two sites were established.

Estimated fluxes through Lancaster Sound are listed in Table 1 and plotted in Figure 6. The reference value for fresh-water is 34.8 and that for heat is -0.1ºC; the latter is an estimate of the average temperature of Arctic outflow through Fram Strait (Aagaard and Greisman, 1975). The 6-year mean heat flux is -4.1 TW (1 TW = 10^{12} W), which appears to indicate a net heat gain by the Arctic via this outflow. However relative to ice, which can exist in equilibrium with typically saline surface water at -1.7°C, even the negative values of heat flux in the table might reasonably be viewed as losses from the Arctic. Volume flux has a 6-year mean of 0.7 Sv, but yearly values span 0.4-1.0 Sv. There is a strong seasonal cycle (Figure 7), ranging between low values in autumn and winter (0.2 Sv) and high values in summer (1.1 Sv). The fresh-water flux is typically about 1/15 of the volume flux – 6-year mean of 48 mSv [1510 km^3/y] – and has a similar seasonal cycle. The range of variation in annual means is 36 mSv [1140 km^3/y].

Atmospheric variability is one possible driver of flow variability in Lancaster Sound. Figure 8 displays an obvious co-variation of 12-month running averages of the NAO Index and of fresh-water flux through Lancaster Sound; the former has been delayed by 8 months. One possible linking mechanism is the oceanic response to AO, mediated primarily via Ekman pumping and via lateral displacement of the Beaufort gyre. The associated cycle in the ocean circulation pattern has been labelled the Arctic Ocean Oscillation by Häkkinen and Proshutinsky (2004). Under this interpretation, the 8-month lag of the flow surge in Lancaster

Sound could represent the spin-up time of the AOO. The possible role of the AOO in forcing Canadian Arctic through-flow is discussed further in the section of chemical tracers.

One goal of present study is the demonstration of a minimal array of moored instruments that could monitor fluxes through Lancaster Sound over the long term with help from numerical ocean models. The relative magnitudes of flows at three locations in the southern half of the section have already been discussed. The lower panel of Figure 5 shows that the upper ocean flow 22 km from the southern shore was close to the average of values from all the three sites during a 3-year period of trial. This demonstration is the basis of a proposed flux-monitoring installation 22 km from the southern shore in 275 m of water. Moored here would be a 300-kHz ADCP at 75 m to measure upper-ocean current and ice drift, a bottom-mounted 75-kHz ADCP (with pressure sensor) to measure deep current, an IPS at 50 m to measure ice draft, temperature-conductivity recorders at several depths below 50 m and an ICYCLER to determine profiles of temperature and salinity in the upper 50 m and a pressure gauge.

Ultimately, if Canadian Arctic through-flow is found to respond predominately to barotropic forcing, then precise, geodetically referenced sea-level stations around the Canadian Archipelago could provide the information needed for numerical models to determine the oceanic fluxes.

8.3 Structure of flow in Hell Gate/Cardigan Strait

Successful year-round use of acoustic Doppler profiling sonar in the Arctic (Melling et al. 1995) has stimulated new initiatives in measuring flow within the Archipelago. An ADCP was deployed on one of two moorings in Smith Sound during the North Water Project in 1997-98. Despite various technical problems, including poor compass performance (H ~ 3300 nT) and weak echoes during winter, data were acquired for 12 months at 20-100 m near the Canadian shore (Melling et al. 2001).

In 1998, Fisheries and Oceans Canada began a study of current in Cardigan Strait with two goals that are fundamental to the successful measurement of fluxes through the Archipelago: 1) a reliable and cost-effective method of measuring current direction near the geomagnetic pole, 2) a better knowledge of the spatial structure of Arctic channel flows.

Cardigan Strait also has advantages as an experimental site. Because it has simple geometry and is only 8 km wide (Figure 9), the through-flow can perhaps be resolved at the internal Rossby scale using a modest array of instruments. Mixing by strong tidal currents (2 m/s) may weaken the density stratification and reduce the importance of the difficult-to-measure baroclinic component of flow. Strong tides provide a key to measuring current direction in the Canadian Arctic because tidal ellipses in this narrow strait are necessarily strongly eccentric and parallel to the Strait's axis. Nearby Hell Gate is an experimental control with half the width and contrasting 'dog-leg' geometry.

The study in Cardigan Strait was planned in phases of two-year duration. The objective of the first phase, 1998-2000, was evaluation of a new torsionally rigid mooring for ADCPs; that of the second was investigation of co-variability between flows in Cardigan Strait and in Hell Gate; that of the third was a look at the cross-sectional structure of flow through Cardigan Strait. In response to presently ambiguous results, the third phase has been continued beyond 2002-2005.

A unique mooring (Figure 10) was designed to meet the special challenges of this environment. It was torsionally rigid to keep the ADCP on a fixed geographic heading throughout the deployment; a universal joint in the backbone allowed the mooring to stand upright regardless of seabed roughness and slope. The ADCP itself was mounted in gimbals to remain zenith-pointing during lay-over of the mooring in strong current. The mooring rose less than 4 m from the seafloor so as to minimize its sensitivity to the drag from current and its vulnerability to icebergs. The mooring was designed to freefall from the surface, enabling its expeditious deployment in fast current and drifting ice; heavy chain arranged in loops as part of the deadweight anchor cushioned the shock of landing at 3 m/s.

Phase 1 provided a clear demonstration of the value of the new mooring, which was over the side and deployed in 30 s, survived impact at the seabed and held the ADCP within ±1° of upright in 2 m/s current and at constant heading for two years. The latter result justifies our reliance on a tidal-stream analysis of the recorded data to infer the ADCP's orientation. Current were measurable using backscattered sound to a range

of 100 m from early July to late January, but the effective range shrank to about 70 m for three months (April through June) when echoes were weak. The strong diurnal variation of echoes implies a biological explanation for the weak back-scatter in late winter. During the second phase, our trial with a 75-kHz ADCP was successful in providing current profiles to the surface (185-m range) in all seasons.

Annual mean currents at 3 locations across Cardigan Strait are shown in Figure 11. Measurements were made on the western slope during August 1998-2000, on the central axis during August 2000-2005 and on the eastern slope during August 2002-2004. The observations reveal uniform current in the middle depth range and sheared flow near the seafloor and the surface. Benthic drag or hydraulics at the sill may influence the lower layer and baroclinicity or wind action the upper. The small year-to-year variation between 1998 and 1999 (western slope), between 2000 and 2001 (channel axis) and between 2002 and 2003 (both eastern slope and channel axis) initially prompted an interpretation that differences between sites were indications of spatial structure in the flow. For example, the left and centre panels of the figure (data not synoptic) suggest a halving of speed in only 2.4 km; this dramatic gradient raises doubt about fluxes calculated using data from a single site in this 8-km wide channel. However, on presumption that data from 1998-2002 provided a valid representation of a constant spatial structure in the flow, we estimated volume flux of 0.2 Sv and 0.1 Sv through Cardigan Strait and Hell Gate (2000-2002 data not shown), respectively.

Prolonged observation has provided new perspectives. Although annual mean current was much the same for 2000 and 2001 and for 2002 and 2003, the annually averaged value span a three-fold range in value over 5 years. Clearly our early assumptions regarding a static cross-sectional variation and temporal constancy are invalid. Moreover, during 2002-2004, the mean (southward) current along the eastern slope of the Strait was about 50% stronger than the mean on the channel axis and Figure 11 indicates that flow along the western slope is also stronger than on the axis. This pattern of cross-channel variation is not consistent with a wall-bounded buoyancy current following the western slope or with a frictionally controlled flow wherein flow would be fastest along the axis. We conclude that observations at more than a few locations are required to measure fluxes even in a channel as narrow as Cardigan Strait.

Results concerning seasonal variation in current are ambiguous; some data reveal an obvious annual cycle and some do not. One of the more definitive records, acquired on the eastern slope of Cardigan Strait during August 2002 to 2004, is plotted in Figure 12. There is a strong Arctic outflow from January through September in both years (strongest in June), but during the autumn and early winter the average flow is weaker and the direction of flow reverses at times. This cycle is roughly in phase with that reported from Lancaster Sound as an average over 6 years of measurement. If this result survives more thorough analysis it will lend credence to a common forcing mechanism for both gateways, perhaps a seasonally varying gradient from the Canada Basin to Baffin Bay that is weakest in the late autumn and strongest in early summer.

The difficulty of calculating the flux of volume through Cardigan Strait and Hell Gate has just been described. The calculation of fresh-water flux as the covariance of flow velocity and salinity anomaly integrated across the channel section is a greater challenge. One part of the challenge is the delineation of the current field; measurement of the time-varying cross-section of salinity is the other. Strong hydrodynamic drag from current (up to 3 m/s in Hell Gate) effectively precludes the use of conventional taut-line moorings to suspend temperature-conductivity recorders at fixed depths. Moreover, hydrographic fields are strongly forced by tidal flow over the sloping topography of the Straits. At fixed depth near the seafloor, where temperature and salinity are presently being measured, the range in the value of these parameters over a tidal cycle is comparable to the range in values that might be measured via an instantaneous CTD cast from surface to seabed. This implies a large contribution to the fresh-water flux from covariance at tidal frequencies. The implied necessity to resolve variation of the salinity section at these frequencies cannot be met with present technology.

8.4 A snapshot of flux via Nares Strait

LeBlond (1980) proposed that the generally cyclonic circulation of icebergs across the mouth of Lancaster Sound was a manifestation of buoyancy forcing related to narrow boundary currents of low salinity. Early direct observations of current revealed an approximate geostrophic balance of flow and cross-channel

pressure gradient (Prinsenberg and Bennett, 1987; Sanderson, 1987) on a scale (10 km) consistent with the internal Rossby radius of deformation.

In August 2003, a team on USCG Healy completed simultaneous surveys of current and salinity in Nares Strait. Flow data were acquired at high resolution using vessel-mounted acoustic Doppler current profiler (ADCP) and conventional hydrographic casts provided temperature and salinity (and therefore density) at 5-km spacing on selected sections. A notable feature of the salinity and density sections was the spreading of isopycnals at about 130-m depth within 10-km of Ellesmere Island (Münchow et al., 2006): isopycnals above this depth sloped upward toward the coast whereas those below it sloped downward. Such hydrographic structure is indicative of a sub-surface baroclinic jet against the western slope of the channel. A weaker feature of similar width was measured near the Greenland coast.

Healy's ADCP operated using a 75-kHz, hull-mounted, phased array. Echoes received at 2-second intervals were processed to yield a vertical profile of velocity relative to the ship. The ship's motion was derived from an independent bottom-tracking pulse (or via high precision GPS tracking) as described by Münchow et al. (2006). Because sonar beams were directed obliquely downwards, velocity was not measured in the lowest 15% of the water column where there is interference from a bottom echo received via beam side-lobes. Also, we lack data for the uppermost 25 m because the hull-mounted transducer was 8 m below the surface, signals from the first 10 m of range were obscured by ring-down of the transmitter and the sonar pulse averaged flow over 15 m in range.

Measured current was the sum of tidal and sub-tidal components, both of which varied with the position of the ship and with time. Sub-tidal current was masked in each instantaneous measurement by tidal flow of as much as twice the magnitude. However, the tidal contribution can be removed from each observation via collective analysis of the group of observations at different places and times. We tried two independent methods. For the first, we subtracted from measured values the tidal current prediction generated by a barotropic model for the time and location of the observation (Padman and Erofeeva, 2004). For the second, judged more appropriate when estimating surface-intensified fresh-water flux, we fit oscillations at tidal frequencies to measured velocities separately at each depth; this method allows a vertical variation in the tidal current.

The continuous ship-based measurements of current easily resolved the internal Rossby radius, which is the spatial scale of baroclinic structure. The along-channel flow at sub-tidal frequency was observed to be spatially coherent with a Rossby number of 0.13, indicating near-geostrophic balance. Approximately one third of the total volume flux was associated with cross-channel slope of the sea surface (barotropic mode) and two-thirds with across-channel slope of isopycnal surfaces (baroclinic mode).

One section at 80.5ºN (Figure 13) was measured repeatedly over several tidal cycles. The sub-tidal flow was southward with much of the flux in the western half of the channel above 200-m depth. The principal feature was a sub-surface jet that peaked at 30 cm/s about 12 km from the Ellesmere coast. The calculated net flux of seawater during the several days of observation was 0.8±0.3 Sv from the Arctic towards Baffin Bay. The southward net flux of fresh water was 25±12 mSv [790 km^3/y]. Both values, but especially the latter, are sensitive to our estimate of current speed in the uppermost 30 m of the water column, which could not be measured. The high sensitivity of fresh-water flux to surface current reflects the low salinity of surface water, which strongly weights the flow speed of this layer on integration. The confidence limit on fresh-water flux is the difference between results using two different assumptions: for a lower bound, fresh-water flux in the top 30 m was completely neglected; for an upper bound we assumed uniform flow in the upper layer equal to the average current in the 18-48-m layer (top 2 bins).

A second section with good observational coverage was completed in Robeson Channel. This 2003 survey encompassed the locations where current was measured for 6 weeks in the spring of 1971. The sparse 1971 array of 3 sites within the 25-km transect is the source of the widely cited 0.6±0.1 Sv volume flux for Nares Strait (Sadler, 1976); in these observations, more than 50% of the calculated flux was associated with a single instrument at 100-m depth near Ellesmere Island. Figure 14 shows the locations along the track of USCGC Healy where current profiles were measured during 7-11 August 2003; the coordinate axes associated with along and cross-channel flow are also shown. The observations were de-tided using tidal

predictions (Padman and Erofeeva, 2004), then averaged at each level within bins spanning 1 km across the channel and 50 km along it. Figure 15 is a cross-section of the along-channel current, which shows the dominant feature to be a southward subsurface jet peaking at 0.4 m/s only 2 km from Ellesmere Island. The maximum speed was at 150 m, where the jet spanned about 10 km of the section. Current through the eastern part of the section was weaker, 0.05 m/s, and northwards. The calculated flux of volume through this section was also about 0.7 Sv in early August 2003, with the principal part within baroclinic subsurface jet on the Ellesmere side.

Prior to and during the survey in 2003, winds were persistent from the southwest (towards the Arctic), promoting down-welling on the Greenland side. Because the subsurface jet below 50-m depth runs counter to wind forcing, atmospheric conditions may have weakened the down-channel flow relative to that associated with more typical airflow from the northeast. Three-year time series from Doppler sonar recently recovered from Nares Strait reveal a strong modulation of current at periods typical of synoptic meteorological forcing (Figure 16). How the data from the surveys of August 2003 fit into this strong pattern of variability has yet to be determined. Nonetheless, the volume out-flux through Nares Strait at this time was comparable to the long-term average inflow to the Arctic through Bering Strait (0.8 Sv); the fresh-water out-flux was about half the estimated inflow through Bering Strait (Woodgate and Aagaard, 2005).

The close correspondence of our volume flux and that of Sadler (1976) is likely fortuitous. The data from Sadler's instrument at 100-m depth close to Ellesmere Island have been viewed with suspicion when compared with weaker flows elsewhere in the section. However with hindsight based on the 2003 data, it is likely that this instrument was optimally positioned to capture flow within the sub-surface jet. By inference this jet is likely a persistent circulation feature in Nares Strait.

8.5 Insights from simulation of Canadian Arctic circulation

Numerical models of fresh-water and ice movement through the Canadian Archipelago face formidable challenges. Principal among these are: 1) the scarcity of data to represent the three-dimensional structure of temperature and salinity and its seasonal variation; 2) the difficulty of resolving necessary detail in the many small but important passages while maintaining a correct dynamical interaction between the modelled domain and bordering seas; 3) the weakness of sea-ice models in representing ice drift through channels, including the appearance and break-up of fast-ice and its influence on oceanic through-flow; 4) realistic wind forcing of oceanic circulation. Until these challenges are met, our preoccupation is the realistic simulation of present conditions. Predictions of flow under future changed climate are fraught with uncertainty.

Nonetheless, there has been notable progress in the numerical simulation of fresh-water and ice movements through the Canadian Archipelago in recent years. Model-based flux estimates for seawater volume and fresh water are converging and models of pack-ice dynamics in island-studded waters have improved.

Advances have emerged from modern coastal-ocean models that have been implemented at high spatial resolution within the Canadian Archipelago. One model, Fundy, is linear and harmonic and a second Quoddy is non-linear and prognostic. The models have been built around the finite element method to best represent the geographic complexity of the area. In the present (2006) implementation the horizontal triangular mesh has 76,000 nodes and 44,000 elements, with resolution ranging from 1.1 km in narrow straits to 53 km in Baffin Bay (Figure 17). The vertical coordinate is resolved via a hybrid mesh with fixed levels over the upper 150 m, where the vertical stratification is strongest, and terrain-following computational surfaces at greater depths. The gridded density field has been developed iteratively, with the horizontal correlation scale inversely dependent on the density of hydrographic observations and directly proportional to the speed and orientation of calculated tidal flow. Fields of potential temperature and salinity for two seasons, summer and late winter, have been constructed from observational archives that span four decades. At present, sea ice appears only via a retarding effect on through-flow appropriate to the season; in other respects it is passive.

The tides are important to circulation within the Canadian Archipelago. They drive mixing and dissipation and control the boundary stresses (drag) in confined waterways. The properties of the tide vary with ice cover particularly near amphidromes where small changes in the amplitudes of incident and reflected waves can have a large impact on phase (Prinsenberg, 1988; Prinsenberg and Bennett, 1989). Dunphy et al. (2005)

have computed a tidal mixing parameter based on modelled tides in the Archipelago. A map of this parameter reveals the regions of most intense tidal influence on mixing (Figure 18). Within the fast-ice zone of the Archipelago, these areas correspond closely to locations of wintertime polynyas. The dramatic inhomogeneity in tidal influence implies differences in water-mass evolution via mixing, heat loss and freeze-thaw cycles during through-flow, depending on the path taken.

There are three runs involved in the simulation of the equilibrium through-flow. In the first, Fundy provides initial fields of sea-surface elevation and velocity from gridded fields of temperature and salinity. In the second, Quoddy is run diagnostically to incorporate tides and non-linear effects. The third run is prognostic. The simulations run for ten days during each of the two observation-rich seasons, March-April and August-September. For sea-surface elevation along the inflow boundary, average June-August values over 52 years have been used. These were computed using an updated version of the large-scale ocean model described by Holloway and Sou (2002). The value varies along the boundary and has an average value of about 0.1 m.

Not surprisingly, the diagnostic model reveals that the partition of through-flow among available pathways depends on the elevation difference between the Arctic Ocean and Baffin Bay and on baroclinic pressure gradients (viz. the distribution of temperature and salinity). For a representative 10-cm difference in sea level, the models yield a mean total through-flow of 0.9 Sv in summer (Kleim and Greenberg, 2004). This value is smaller than numbers derived from observations (Melling, 2000) but larger than the Steele et al. (1996) value derived from a simple ice-ocean model driven by observations of ice drift and concentration. Of the modelled total flux, 46% via passes Nares Strait, 20% via Cardigan Strait/Hell Gate and 34% via Lancaster Sound (Table 2). The model indicates that outflow via Lancaster Sound is supplied mostly from the Sverdrup Basin, with little contribution from Viscount Melville Sound and channels to the south (Figure 19). This interesting outcome is consistent with observations reported by Fissel et al. (1988). The relationship between flux and sea-level difference is linear in the models (wherein hydrographic fields are fixed): a 5-cm increase in the sea level of the Arctic relative to Baffin Bay doubles the flux of volume.

The net volume flux reflects a balance between the barotropic pressure gradient, which drives water from the Arctic Ocean toward Baffin Bay, and the baroclinic pressure gradient which forces flow in the other direction. This is clear from Table 2 where the diagnostic result and that of a barotropic calculation using the same sea-surface elevation along the Arctic boundary are compared: the volume flux associated with barotropic forcing alone is five times larger. Clearly the baroclinic mode is an important aspect of circulation in the Canadian Archipelago. However, this result should not be viewed as an accurate measure of the relative contributions of the barotropic and baroclinic modes to flux. The ratio is suspect because it was derived using the diagnostic mode wherein the density field was specified (and of necessity grossly smoothed) and unresponsive to the circulation. Only a fully prognostic model can reveal whether this is a problem.

The diagnostic calculation has also provided values for the fluxes of fresh water and heat associated with the seawater volume flux. Values provided in Table 2 are subject to the cautions raised in the preceding paragraph. Typically, the model totals for all three routes of through-flow are approximately equal to values derived from observations in western Lancaster Sound alone (see Table 1), namely about 50 mSv (re 34.8) for fresh water [1580 km^3/y] and -3.4 TW (re -0.1ºC) for heat.

There have been few modelling studies with spatial mesh sufficiently fine to represent baroclinicity adequately within the narrow channels of the Canadian Archipelago. The coupled ice-ocean model of the US Navy Postgraduate School, which has one-twelfth degree resolution (about 9 km), has been used for pan-Arctic simulations of the period 1979-2002 (Williams et al. 2004). The results indicate that the Canadian Arctic through-flow is the greater contributor (relative to Denmark Strait) of oceanic fresh water to the North Atlantic. According to the simulation, the fresh-water flux through the Archipelago has increased over the period studied, a trend that has perhaps contributed to the well documented freshening of the Labrador Sea.

The goal of future work is a prognostic model with time evolving fields of temperature and salinity. This is not a trivial undertaking, particularly on a terrain-following mesh, and methods with acceptable truncation error have been sought for many years. Such capability is essential for realistic simulation of baroclinic effects, including fresh-water and heat fluxes. An increase in resolution is also desirable, best accomplished

for this area using the finite element method. The present best resolution is 1.1 km, barely adequate to represent important channels such a Hell Gate (4 km), Cardigan Strait (8 km) and Fury and Hecla Strait (1.8 km). Ocean circulation models need to be forced using wind fields that adequately reflect the important influence of topography and boundary-layer stratification on the mesoscale. Lastly, there is need for a realistic and fully interactive ice dynamics model; not only is pack ice an important element of ocean dynamics, but moving ice can represent an appreciable fraction of the fresh-water flux, by virtue of its rapid movement and low salinity. The ice element may take on an increased importance in total fresh-water flux with a warmer climate, wherein ice may be mobile for a much larger fraction of each year (Melling, 2002).

8.6 Ice flux across the Canadian polar shelf

The geography of the Canadian Archipelago is too complex for effective use of satellite-tracked drifters to measure the through-flow of pack ice. Methods based on the tracking of features in sequential images from satellite-borne sensors are better suited to the task. Microwave sensors provide the least interrupted time series of ice flux at key locations because they are relatively unaffected by cloud and wintertime darkness. However, the tracking of ice movement may be error-prone at times when ice features have poor contrast or when the pack is rapidly deforming as it moves; the latter is a common circumstance during rapid drift through narrow channels.

The displacement of sea ice over the interval between two images is derived by the method of maximum cross correlation (Agnew et al., 1997; Kwok et al., 1998). The technique works with sub-regions or patches on the two images that are 5-50 pixels on a side, depending on resolution. The underlying premise is that difference between consecutive images result from a simple displacement, the same for all features. Any additional rotation and straining of the ice field or creation of new ice features (e.g. leads) degrade the correlation.

Two long-term studies of ice movement through the Canadian Arctic have been completed. One used scenes acquired by synthetic-aperture radar at 0.2-km resolution (Radarsat: Kwok, 2005; Kwok, 2006) and the other utilized images from a passive microwave scanner, which resolves ice features at approximately 6-km resolution (89 GHz AMSR-E: Agnew et al., 2006). Both approaches yield estimates of ice displacement and ice concentration at intervals of 1-3 days, constrained by the interval between repeated orbital sub-tracks.

The utility of AMSR-E is marginal in some parts of the Archipelago where channels are only a few pixels wide. Moreover, the 89-GHz channel is of little value during the thaw season (July-August) when the wet surface of the ice and high atmospheric moisture degrade image contrast; data acquired during the shoulder-months of June and September may also be poor at times. Microwave radar produces images of better contrast than microwave scanners during the thaw season, but the identification of floes and ice features in thaw-season scenes from Radarsat can be challenging.

The flux estimates derived from microwave-emission images only incorporate ice motion that occurred during the colder months (October-May or September-June). Since this period overlaps significantly with fast-ice conditions within the Canadian Archipelago, the months of most active ice movement may have been missed. The flux estimates derived from Radarsat nominally span the entire year. However, it is noted that feature-tracking algorithms return a null result (low correlation) when the quality of images is poor or ice-field deformation is large; this fact may contribute a low bias to average displacement during the summer, when image contrast is poor and low ice concentration permits rapid movement and deformation of the pack.

Radarsat transmits microwaves and detects the energy back-scattered from the rough surface or upper few centimetres of the ice; it is not sensitive to ice thickness. AMSR-E detects natural microwave emission at several frequencies and polarizations, which can be manipulated to yield information on ice type and concentration. In general, satellite-based data on ice movement must be augmented by ice-thickness values from other sources if the flux of ice volume and fresh-water are to be estimated.

Kwok et al. (1999) calculated an area budget for Arctic multi-year ice during 1996-97 using observations made from space by microwave scatterometer (NSCAT). They estimated an annual outflow from Nares Strait of 34 x 10^3 km^2 by mapping multi-year ice in northern Baffin Bay, presumed to have arrived here via Smith Sound. Subsequently, Kwok (2005) has used Radarsat images over a 6-year period (1996–2002) to

measure directly the drift of ice through a 30-km wide gate at the northern end of Robeson Channel (Figure 20). During these years, the average annual flux of ice from the Lincoln Sea into Nares Strait was 33 x 10^3 km^2, with an inter-annual span of ±50%. There was a strong annual cycle in ice drift, with the bulk of the transport during August through January; ice is typically fast in Nares Strait between mid winter and late July. On assumption of 4-m thickness, the average volume flux was 130 km^3/y [4 mSv].

For the years 1997-98 to 2001-02, Kwok (2006) has estimated ice-area transport across the main entrances to Canadian Archipelago from the west (Figure 20): Amundsen Gulf, M'Clure Strait, Ballantyne Strait plus Wilkins Strait plus Prince Gustaf Sea (cf. Queen Elizabeth Islands south) and Peary Channel plus Sverdrup Channel (Queen Elizabeth Islands north). His results are summarized in Table 3. On average during the 5-year study, Amundsen Gulf was a source of ice for the Arctic Ocean. Since the Gulf was ice-free during the summer, as typical, most of the export would be first-year ice leaving during autumn and winter. On assumption of 1-m average thickness (perhaps high because the gate traverses the Bathurst polynya), the average export was 85 km^3/y. There was also an average export of ice from M'Clure Strait to the Beaufort Sea, although in smaller quantity and with occasional reversals (there was net import from the Beaufort in 2000). The average export was 80 km^3/y, on assumption of 4-m average thickness (McLaren et al., 1984). Only the entry points to the Sverdrup Basin accepted a net influx of ice to the Canadian polar shelf, but the amount was small (8 x 10^3 km^2/y or 7 km^3/y if ice was 3.4 m thick). This net influx is consistent with the analysis of Melling (2002), although its value is only about 20% of that implied by Melling's analysis.

The analysis has been extended to the cold months of 2002-03 to 2005-06 using AMSR-E (Agnew et al., 2006). The pattern of flux, with export from Amundsen Gulf and M'Clure Strait and import into the Sverdrup Basin, was continued during this period. However, the average out-fluxes from Amundsen Gulf and M'Clure Strait during this 4-year period (14 and 5 x 10^3 km^2/y) were smaller than during the preceding 5-year period (85 and 20 x 10^3 km^2/y) and the influxes to the Sverdrup Basin (30 and 6 x 10^3 km^2/y) were larger (6 and 2 x 10^3 km^2/y). There is obviously strong inter-decadal variability, as inferred by Melling (2002), which may respond to cycles in atmospheric circulation; it may also be that ingress of pack ice to the Sverdrup Basin was easier after the extensive loss of old ice within the Archipelago in 1998.

On the other side of the Canadian Archipelago, ice generally moves from the Canadian polar shelf into Baffin Bay. Agnew et al. (2006) have also used images acquired via AMSR-E to estimate ice flux into Baffin Bay during the colder months of 2002-03 to 2005-06: annual average fluxes were 48, 10 and 9 x 10^3 km^2/y via Lancaster, Jones and Smith Sound, respectively. The associated fluxes of volume were 49, 10 and 9 km^3/y per metre of ice thickness.

Agnew and Vandeweghe (2005) have also calculated the ice flux during 2002-04 through a gate across central Baffin Bay; the average over the 2-year interval was 690 x 10^3 km^2/y southward. Clearly the efflux of ice from the Canadian polar shelf during the last decade has been larger than the influx, implying that much of the ice exported to the Labrador Sea has been formed there and not in the Arctic Ocean itself. Moreover, the southward flux of ice through Baffin Bay actually exceeded that through Fram Strait over the same period in terms of area (590 x 10^3 km^2/y: Agnew and Vandeweghe, 2005). However because the Fram Strait flux is primarily old ice and that the Baffin flux is primarily seasonal, the export of ice volume through Baffin Bay is probably the lesser.

Table 4 summarizes the ice flux values discussed here.

8.7 Terrain-channelled wind and oceanic fluxes

The probable cause of the persistent flow of seawater through the Canadian Archipelago into Baffin Bay is a drop in sea level of 0.1-0.3 m (Muench, 1971). However, an accompanying flow of ice through the narrow waterways is strongly constrained by material stresses within the pack. In most channels, high ice concentration and low ice temperature during the cold season are sufficient to halt ice drift, despite continued strong forcing. The first consequence is cessation of fresh-water flux via moving ice. The second is increased drag on oceanic flows and their isolation from stresses exerted by wind.

Pack ice in Nares Strait usually consolidates in winter behind an ice bridge in Smith Sound (Agnew, 1998). Consolidation can occur any time between November and April, and may occur in stages, with bridges

forming consecutively in Robeson and Kennedy Channels and Smith Sound, perhaps to collapse a few weeks later or perhaps to remain as late as August. Such variability suggests that the fast-ice regime of Nares Strait is of marginal stability in the present climate, flitting between the permanent mobility typical of Fram Strait and the reliably static winter ice of the western Archipelago.

It is plausible that topographically amplified winds in Nares Strait contribute to the intermittent instability of fast ice in the channel. However because there are no systematic long-term observations of wind in the area, present insights have been derived via numerical simulation (Samelson et al., 2006) using the Polar MM5 mesoscale atmospheric model (Bromwich et al., 2001). This is a version of the Pennsylvania State / NCAR MM5 (non-hydrostatic, primitive-equation, terrain-following, full moist physics) which has been optimized for the polar environment (Cassano et al., 2001; Guo et al., 2003). The configuration is triply-nested, from 54-km to 18-km to 6-km grids. It has been run daily at Oregon State University since August 2003 in a 36-hour forecast mode, with initial and time-dependent boundary conditions taken from the operational AVN model of the US National Center for Environmental Prediction.

Strong radiational cooling at the surface in Nares Strait frequently creates a stable planetary boundary layer in winter, wherein wind may be strongly channelled by surrounding mountains. The mesoscale model commonly generates an intense boundary-layer jet at elevation below that of the confining terrain. Moreover, the along-channel wind speed is well correlated with the difference in sea-level pressure along Nares Strait (Samelson et al., 2006). The along-channel balance indicates that the atmospheric jet is an ageostrophic response to orography. The drop in sea-level pressure along the 550-km long strait can exceed 25 mb, with simulated winds reaching 40 m/s at 300-m elevation.

Meso-scale processes are clearly influential in accelerating airflow through Nares Strait: high terrain on both sides, the unusual length of the channel and its narrow width isolate air flow from the synoptic-scale geostrophic constraint; the strong ageostrophic response to pressure gradient is only weakly damped by momentum transfer through the stable boundary layer; the ageostrophic response is locally amplified by effects of varying channel width. Moreover regional synoptic climatology is a contributing factor because Nares Strait is a short-cut between two different synoptic regimes, the Polar high and the Icelandic low. Figure 21, depicting the regional variation in sea-level pressure from the MM5, clearly reveals both synoptic-scale and mesoscale factors: the large difference in pressure between the Lincoln Sea and Baffin Bay and the two zones of steep pressure gradient and strong along-channel wind, in Kennedy Channel and in northern Baffin Bay. The probable along-channel force balance involves the pressure gradient, inertia and friction while the cross-channel balance is geostrophic (on the mesoscale). Boundary stress likely fades to insignificance above a few hundred meters, leaving an inviscid balance in the upper part of the jet.

The dynamical explanation for the wind maxima at two locations, where Kennedy Channel widens into Kane Basin and again where Smith Sound widens into Baffin Bay may be super-critical flow. This phenomenon is known to create similar expansion fans in summer in the lee of capes on the US west coast (Winant et al., 1988; Samelson and Lentz, 1994). Pressure gradients develop as the inversion-capped marine boundary layer thins where the channel widens; these gradients in turn force ageostrophic acceleration.

Empirical orthogonal functions computed from monthly averages of simulated airflow and surface stress over a 2-year period (Figure 22) show that the time-dependent flow has a spatial structure very similar to that of the mean flow, shown for January 2005 in Figure 21. The annual cycle was energetic during this particular period: the average airflow alternated between strongly southward during October through January and northward in July and August.

Variance in the synoptic band of frequency was suppressed by the monthly averaging applied in the preparation of Figure 22. Nonetheless, this band is very energetic in Nares Strait. Figure 23 displays the along-channel surface wind for a one-year period. Values have been derived from the along-channel difference in sea-level pressure (Carey Islands minus Alert) using the regression line calculated by Samelson et al. (2006), but comparable fluctuations are apparent in simulated winds.

Simulations of mesoscale atmospheric flow within the Canadian Archipelago have been focussed to date on Nares Strait. However, it is likely that each of the six constrictions to through-flow in the oceanic domain – Nares Strait, Hell Gate, Cardigan Strait, Lancaster Sound, Bering Strait and Davis Strait – have some impact

on the speed and direction of winds. The intensity of mesoscale influence likely differs within the group, since the straits encompass a wide range of dimensions in terms of height of terrain (200-2000 m), width of strait (8-350 km), length of strait (0-550 km) and latitude. The latter may influence boundary-layer stability through its direct and indirect effects on insolation, surface albedo and surface emissivity. Based on our presently incomplete understanding of these effects within Nares Strait, we rank the straits in the following sequence of decreasing sensitivity to wind amplification on the mesoscale: Nares Strait, Cardigan Strait/Hell Gate, Lancaster Sound, Davis Strait, Bering Strait.

8.8 Geochemical identification of sources for Canadian Arctic outflow

Although the primary indicator of fresh water in the ocean is salinity, a number of trace chemical constituents can provide insight into fresh-water origin and transport within the Arctic. Recent studies that illustrate the application of chemical tracers to Arctic fresh-water issues have been published by Cooper et al. (1997), Jones et al. (1998), Smith et al. (1999), Schlosser et al. (2000), Ekwurzel et al. (2001), Amon et al. (2003), Jones et al. (2003), Taylor et al. (2003), Alkire et al. (2006), Falkner et al. (2006), Yamamoto-Kawai et al. (2005), Yamamoto-Kawai et al. (2006) and Jones and Anderson (2007). Exploited dissolved trace chemicals include nutrients, molecular oxygen, alkalinity, chlorofluorocarbons, natural and artificial radionuclides, barium and other trace metals, organic matter and heavy isotopes ^{18}O and ^{2}H in water molecules.

The interpretation of the first exploratory sampling of tracers was constrained by poor geographic coverage. Data from several expeditions, perhaps spanning several years, were typically aggregated or averaged to draw maps of tracer distributions. Interpretation was necessarily based on the assumption of steady ocean circulation. Increased effort in data collection over the last decade has permitted a more rewarding focus on temporal variability. Here we discuss new knowledge emerging from tracer hydrography in the western hemisphere of the Arctic, with particular attention to temporal variability in the relative contributions from various sources of fresh water. In future years, a significantly improved understanding should emerge from the time series of strictly comparable data that are now being produced.

The interpretation of oceanographic tracers in the North American Arctic presents special challenges. For example, the region encompasses a range of sea-ice environments from year-round ice cover, through seasonal ice zones to ice-free seas. Simple assumptions applied elsewhere regarding the impacts of biology and ventilation on tracer concentrations are often inappropriate. Interpretation of tracer distribution can be ambiguous: for example, Baffin Bay receives Arctic waters via two paths, from the north via the Canadian Archipelago and from the south via the West Greenland Current. Moreover, fresh water with large and variable $\delta^{18}O$ anomalies from melting ice sheets in Greenland and northern Canada (which also contribute glacial flour) increases the complexity of geochemical interpretation.

Dissolved nutrients and oxygen have the longest history among all chemical tracers used in ocean science, in the Arctic as in temperate waters. A relatively high concentration of silicic acid ($[Si] \geq 15$ mmol m^{-3}) has long been known to distinguish waters that enter the Arctic from the Pacific via Bering Strait; this influx can be traced as a relative maximum in dissolved silica concentration (coincident with a maximum in dissolved phosphorus [P] and coupled with a minimum in dissolved oxygen [O_2]) in the halocline (Kinney et al., 1970; Codispoti and Lowman, 1973; Jones and Anderson, 1990). Recent interpretation that additionally utilizes $\delta^{18}O$ has revealed that the dissolved nutrient and oxygen in the Arctic halocline result primarily from the Bering Strait inflow that occurs in winter (Cooper et al., 1997 & 2006). In the sunlit half of the year, biological cycles of growth and decay change the concentrations of dissolved nutrients and oxygen. Biological impact is further accentuated because the Bering Strait inflow is less saline (and therefore closer to the surface) and free of light-obstructing ice cover at this time of year. Thus tracing the movement and fate of Bering Sea water that enters the Arctic during spring, summer and autumn demands ingenuity in geochemical interpretation.

Within the Canadian Archipelago, the earliest reliable cross-sections of dissolved silica were observed in the summer of 1977. The concentration was highest in Lancaster Sound, intermediate in Jones Sound and lowest in Smith Sound. This gradation was taken to indicate that very little water from the Pacific waters reached the Lincoln Sea where it could contribute to the flow through Nares Strait (Jones and Coote, 1980).

This conclusion was revised substantially when the co-variation of dissolved nitrate and phosphate was developed as a discriminant of Pacific from Atlantic-derived waters within the Arctic (Jones et al., 1998; Alkire et al., 2006; Yamamoto-Kawai et al., 2006). De-nitrification of inflowing seawater occurs over the shallow shelves of the Chukchi and northern Bering Seas. This process renders the Pacific inflow deficient in fixed inorganic nitrogen relative to Atlantic water. Within the Arctic Ocean, biological action tends to move the nitrate and phosphate concentrations within each contributing water mass (Pacific and Atlantic) along lines of constant "Redfield-like" slope on a nitrate-versus-phosphate diagram. Mixtures of Pacific and Atlantic waters have concentrations of these two constituents that fall between the source-water reference lines; the position between the reference lines can be used to calculate the relative contributions of Pacific and Atlantic-derived waters to the mixture.

Complications arise with the contribution of water from other sources, such as rivers and melting ice. To a first approximation, however, studies of $\delta^{18}O$ reveal that these interfering contributions are generally less than 10% within the Arctic Ocean (Östlund and Hut, 1984) and that rivers provide nutrients in proportions resembling those characteristic of Atlantic water (Jones et al., 1998). The nitrate-phosphate (N-P) method for discriminating Pacific from Atlantic waters has recently been refined to include the contribution of ammonium and nitrite to the fixed inorganic nitrogen. The quality of the analysis has thereby improved because ammonium is commonly a significant contributor to the Pacific component (Yamamoto-Kawai et al., 2006).

Jones et al. (2003) have applied the N-P method to track the Pacific influence within Arctic outflows through the Canadian Archipelago, Baffin Bay and Davis Strait to the Labrador Sea and through Fram Strait and Denmark Strait. From hydrographic sections measured in August 1997, they concluded that Pacific inflow completely dominated the seawater end member in Barrow Strait and provided at least three quarters of this end member in the topmost 100 m of Jones and Smith Sounds; Pacific water was similarly prevalent that year within 100 km of Baffin Island in Davis Strait. It was detected in diluted (50%) form with somewhat variable extent over the Labrador shelf in 1993, 1995 and 1998 and as far south as the Grand Banks in 1995.

The magnitude of Pacific influence in waters south of Davis Strait may be an over-estimate because de-nitrification likely occurs also in the relatively shallow waters of Hudson Bay. N*[2] is a nutrient-based parameter that has negative value in de-nitrified water. In the North Atlantic values of N* are near zero or positive. Values of N* are negative for Pacific waters passing through Bering Strait and about –12 μM/kg for water in Barrow Strait [Falkner et al., 2006]. Unpublished data from Hudson Bay in the summer of 1982 (Bedford Institute of Oceanography, DFO Canada) reveal water with N* even more negative (-23 to -12 μM/kg). Because the deepest waters of Hudson Bay (S ~ 33.5) are replaced on a time scale of about a decade (Roff and Legendre, 1986), Atlantic water supplied to Hudson Bay via Hudson Strait could be de-nitrified to a Pacific-like signature before re-emergence into the Labrador Sea. Such occurrence would obfuscate the N-P interpretation wherever there is influence from Hudson Bay.

A recent analysis that combines measurements of tracer concentration and current velocity on several sections across Nares Strait is a novel innovation (Falkner et al., 2006). The current measurements by ship-mounted ADCP in August 2003 delineated a southward jet at 100-200 m depth along the western side of Nares Strait; the enrichment of silica and phosphorus in this jet is indicative of origin as wintertime inflow to the Arctic through Bering Strait. Hydrographic sections measured at the same time reveal that Pacific water comprised the entire seawater end member within the topmost 100 m in Robeson Channel at the northern end of Nares Strait, but that mixing during southward transit had diminished the seawater component to a 50/50 mixture of Pacific and Atlantic waters in Smith Sound. Pacific influence in the mixture was appreciably more dilute than at this section in 1987. Subsequent comparison of nutrient measurements in August of various years has revealed considerable inter-annual variability (Figure 24). The magnitude of inter-annual variation in silica is comparable to that proposed as seasonal in the interpretation of a 10-month (autumn, spring to summer) study of dissolved nutrients in the North Water in 1997-98 (Tremblay et al., 2002).

[2] N^* (μM/kg) = $[NO_3] - 16 \cdot [PO_4] + 2.90$. N* was first defined by Gruber and Sarmiento (1997) and modified by Deutsch et al. (2001).

Figure 24 displays measurements of nutrient concentration in Canadian Arctic straits that accommodate both Arctic outflow and inflow from Baffin Bay. The envelopes that enclose these data are shifted toward higher nutrient concentration (viz. greater Arctic influence) in August 1997 than in 1977 and 2003 (Falkner et al., 2006). The simplest interpretation is that the flux of nutrient rich Pacific water (plus meteoric and ice-melt waters mixed with it) was higher in all the straits in August 1997 than in 1977 and 2003. The higher flux occurred just after the prolonged positive anomaly in the Arctic Oscillation Index (AO) during 1989-95.

What is the mechanism via which the AO, which is an expression atmospheric pressure distribution over the Northern Hemisphere in winter, influences oceanic circulation and fluxes in summer? Proshutinsky and Johnson (1997) used a barotropic ocean model to demonstrate that the Arctic Ocean responds to the AO in a basin-wide oscillation with cyclonic and anti-cyclonic anomalies: higher peripheral sea level results from the set-up of low salinity water against the ocean boundary under high AO forcing. A subsequent study was based on a more realistic ice-ocean model was forced by NCEP-reanalysis winds for 1951-2002 (Häkkinen and Proshutinsky, 2004). Various measures of the Arctic Ocean Oscillation, including sea surface height, all co-varied with the Arctic (Atmosphere) Oscillation. During the years of unusually high AO, 1989-96, the model indicated a sustained loss of fresh water from the Arctic Ocean, which had by 1997 created the most negative fresh-water anomaly of the entire 50-year simulation. Although Häkkinen and Proshutinsky (2004) do not comment on whether the exported fresh water passed to the east or to the west of Greenland, the timing meshes with the inference of Falkner et al. (2006) based on geochemical analysis of Canadian Arctic through-flow in 1997. Interestingly, the inflow of Atlantic water was an essential element in the wind-driven barotropic response to the AO; it was the factor most strongly correlated with fresh-water anomalies within the basin. The future will tell whether this view of the Canadian Arctic through-flow is consistent with more complete observational time series now being collected.

Additional trace compounds can be used to distinguish the meteoric (river inflow plus precipitation) and ice-melt components of Canadian Arctic through-flow. For example, Jones and Anderson (this volume) discuss the use of seawater alkalinity for this purpose. Östlund and Hut (1984) pioneered the mass-balance analysis of the seawater isotopic composition in the Arctic to distinguish run-off from ice melt-water as freshening agents. Within the Canadian Archipelago and east of Greenland, a more complicated analysis may be required. As discussed by Strain and Tan (1993), the separation of salt and water by the freeze-thaw process can, in combination with mixing under conditions prevalent in Baffin Bay, generate a seasonal cycle in the $\delta^{18}O$ value for the zero-salinity end-member. The $\delta^{18}O$ values can vary from that typical of summertime precipitation ($\delta^{18}O \approx -10$) to that typical of glacial melt-water ($\delta^{18}O \leq -25$). In the big picture, direct contributions of fresh-water via precipitation and ablation of ice sheets are small relative to those via Arctic rivers ($\delta^{18}O \approx -20$) and Pacific inflow ($\delta^{18}O \approx -1$). However, they may be important in the principal Arctic fresh-water outflows because of proximity to the ice sheets of Greenland and of the Canadian Arctic Cordillera. An ideal analysis would be expanded to incorporate additional tracers and contextual information so that artefacts can be identified.

8.9 Gateway to the Atlantic, Davis Strait

With the exception of about 0.1 Sv that is diverted along the western side of Baffin Island via Fury and Hecla Strait (Barber, 1965; Sadler, 1982), all streams of Arctic water that cross the Canadian polar shelf enter Baffin Bay. These join the cyclonic recirculation of the West Greenland Current (itself fed by Arctic outflow via Fram Strait) to form the Baffin Current. This stream follows the continental slope of Baffin Island and enters the Labrador Sea through Davis Strait.

The properties of Arctic seawater and ice are modified by freezing, thawing, terrestrial and glacial run-off and mixing during their transit across the Canadian polar shelf (more than 1 million square kilometers of ocean area) and through Baffin Bay (an additional ⅔ million square kilometers) to Davis Strait. Although the residence times for through-flowing water and ice are not known, they are likely significantly longer than the most rapid transit (by ice from the Lincoln Sea to Davis Strait), which requires about a year. Ultimately, it is this modified Arctic water mass that affects deep water formation in the Labrador Sea. Davis Strait is a suitable location to measure the sum of all Arctic outflows via routes west of Greenland at a single section just prior to their entry into the deep convection zone.

However, the operation of an array to measure volume and fresh-water fluxes through Davis Strait is not a trivial undertaking. The Strait at its narrowest is about 360 km wide, with more than 200 km of this span deeper than 500 m and maximum depth is close to 1000 m. There is a topographic spur that extends along the axis of the Strait and likely influences flow near the sill. Relative to the internal Rossby scale, the Strait is dynamically wide, admitting small eddies and recirculation that must be resolved to obtain accurate estimates of fluxes. The upper few hundred metres, particularly on the Canadian side, are swept by a broad stream of icebergs moving south with the current, which complicate measurements within the major part of the Arctic outflow. There is a strong counter-flow (the West Greenland Current) on the eastern side of the Strait, with a front, eddies and re-circulation features in the region where the two currents interact over the broad flat sill.

The water masses and circulation within Davis Strait during the ice-free season have been mapped using hydrographic surveys and satellite-based temperature scanners. The bathymetric chart of Figure 25, showing the extent of continental shelf (150 km on the Greenland side) to the 500-m isobath, has an underlay which represents the mean sea-surface temperature for September. Water warmer than 4ºC (fresher than 33) in the Labrador Sea and over the Greenland shelf is carried northward by the West Greenland Current; it is a mixture of Atlantic water with outflow from Fram Strait. Most of this stream turns west and then south along isobaths in the northern Labrador Sea; some continues northward along the Greenland shelf. Vectors in Figure 25 represent depth-averages of measured current; they confirm this inference of northward flow on the Greenland side and the southward flow of Arctic water on the Canadian side.

There are three principal water masses in Davis Strait (Tang et al., 2004): Arctic Water, West Greenland Intermediate Water originating in the Atlantic and Baffin Bay Deep Water (below 800 m). Figure 26 displays their distribution across a hydrographic section measured at 25-km resolution in September 2004. Here West Greenland Intermediate Water is warmer than 2ºC, more saline than 34.5 and extends from the Greenland slope into mid-strait below 50-m depth; a smaller core of this water over the Baffin slope is likely a recently separated filament that is returning southward. Arctic water colder than 0ºC and fresher than 33.5 fills the upper 250 m of the western half of Davis Strait; here the salinity anomaly (re 34.8) is quite large in a thin layer within 50 m of the surface. Both this thin layer and the sharp front that separates Arctic from Atlantic-derived water present significant challenges to measurement.

Hydrographic sections measured recently at high (5-km) resolution by Seaglider[3] illustrate the challenge posed by meso-scale structure within Davis Strait (Figure 27). Even at this fine station spacing, there is plentiful detail in temperature, salinity and geostrophic shear at the limit of resolution; average values of current for the upper 1000 m (estimated from glider navigation) uncover analogous variation. The high-resolution section also reveals the large fresh-water anomaly of the thin surface layer. The movement of this surface layer represents a substantial fraction of the fresh-water flux in Arctic waters (Melling, 2000). Moreover in ship-based surveys, such features are frequently damaged by propeller wash before measurement.

During 1987-90, Fisheries and Oceans Canada maintained an array of conventional current meters (current, temperature, salinity at 150, 300 and 500 m) on five moorings along the 66.25º N (Ross, 1992). The array spanned the deep central trough at roughly 50-km spacing. Because instruments were not placed shallower than 150 m, where iceberg risk is high, the array did not cross the shelves or sample the low-salinity Arctic outflow. In addition, Tang et al. (2004) and Cuny et al. (2005) report low correlations between time series from instruments on different moorings, indicating that the array failed to resolve flows at the scale of variability within the Strait. These shortcomings of the array (gaps in coverage, aliased variance) introduce

[3] Seaglider is a autonomous vehicle developed by the Applied Physics Laboratory / School of Oceanography, University of Washington. It is 2 m long and weighs about 50 kg. It undertakes hydrographic surveys of many months duration, profiling from zero to 1000-m depth by carefully controlling its buoyancy. Seaglider moves by adjusting its attitude so that its flight planes deflect vertical motion (approximately 8 cm/s) into horizontal. Internal navigational algorithms and a reference compass allow the vehicle to fly a specified course at 20 km/day. In ice-free seas, the GPS provides position to the Seaglider at the surface; at the same time, revised instructions, engineering and science data can be transferred via Iridium satellite communications. Capabilities for acoustic navigation and data relay are being developed for use under pack ice in Davis Strait.

large uncertainty in estimating flux. Nonetheless Cuny et al. (2005) moved ahead by assuming that: 1) temperature and the salinity were constant above 150 m when the sea was ice-covered; 2) seasonally appropriate recent or historical data provided valid vertical gradients above 150 m during ice-free months; 3) upper ocean profiles could be estimated by shifting climatological data to match daily values observed at 150 m; 4) measured daily current speed at 150 m provided known motion at a reference level for calculated geostrophic current; 5) values varied linearly between moorings. Fluxes over adjacent continental shelves were ignored. Tang et al. (2004) have used the same data under slightly different assumptions; principally they substituted climatological values for salinity gradient in the upper ocean year-round.

The upper part of Table 5 summarizes volume and fresh-water flux estimates derived from these older data. Values based on the long-term, but under-resolved, direct observations average about 3.1 Sv and 125 mSv [3940 km^3/y], respectively[4] (Loder et al. 1998; Tang et al. 2004; Cuny et al. 2005). Fluxes passing along the Greenland shelf have not been included; Cuny et al. (2005) estimate these as -0.8 Sv and -38 mSv [1200 km^3/y], so that their corrected net fluxes for the entire Strait are 2.3 Sv and 87 mSv [2750 km^3/y]. The hydrographic surveys in September provide better horizontal resolution and include the shelves but are short-term views; the estimates are therefore more variable but also are larger, ranging over 1.5-5.7 Sv and 126-286 mSv [3980-9020 km^3/y]. It is plausible (and consistent with some observations within the Archipelago) that the fluxes might actually be larger in September than in annual average, though this interpretation should be cautious because uncertainty stemming from poor resolution and unknown barotropic transport is large.

The lower part of Table 5 summarizes preliminary flux estimates derived from the ongoing USA-Canada Freshwater Initiative that is acquiring data from a new and larger moored array and hydrographic surveys by ship and Seaglider. The present summary is preliminary, derived from independent perspective of each source of data. Geostrophic calculations referenced to zero at the seabed and averaged over four sections yield volume fluxes of 1.8 ±1.5 Sv and 2.3 ±0.9 Sv for September 2004 and 2005. A simplistic estimate based on data from moored instruments during 2004-05 (including some measurements over the shelves) is an annual mean value of 2 Sv, with large uncertainty. Preliminary estimates of fresh-water flux from the ship CTD survey in September 2004 and the September/October 2005 transects by Seaglider are 93 ±40 mSv [2930 km^3/y], including shelves and 96 ±20 mSv [3030 km^3/y], excluding shelves. These values are smaller than those estimated from data in the late 1980s, but the magnitude of error is unknown and likely large.

The fluxes listed are net values. The West Greenland Current has a northward flow of approximately 2 Sv in Davis Strait, and relative to 34.8 reference salinity it carries fresh-water northward at roughly 60 mSv [1890 km_3/y] (Cuny et al., 2005). Therefore, based on Cuny's numbers, the fluxes southward within the Baffin Current are 4.6 Sv and 150 mSv [4730 km^3/y].

Narrow buoyancy-driven flows analogous to the Alaska Coastal Current may carry appreciable fresh-water during summer within 10 km of the Greenland and Baffin coasts. For example, a coastal current fed by ice-sheet run-off along southeast Greenland apparently transports volume and fresh-water at 1 Sv and 60 mSv [1890 km^3/y] during the thaw season (Bacon et al., 2002). Components of the present observational array may detect such currents but will not likely resolve their extent and rate of transport.

The USA-Canada Fresh-water Initiative is addressing the principal challenges to accurate measurement of volume and fresh-water fluxes through Davis Strait. Among these are: 1) a small baroclinic deformation scale that permits decorrelation of flow variations on a scale of order 10 km; 2) a pronounced concentration of freshwater flux in a thin (25 m) fast-moving surface layer where current and salinity are difficult to measure; 3) the risk to moorings from moving ice keels and icebergs at depths as great as 200 m; 4) the fresh-water flux carried by pack ice. The Initiative has brought new technology to bear on these challenges.

Instruments on six sub-surface moorings measure ice draft (upward looking sonar), ice velocity and profiles of upper ocean current (ASCP) from a relatively safe depth of 105 m, current at specific depths in the lower part of the water column (conventional current meters) and seawater temperature and conductivity from sensors at discrete depths (Figure 28). There are also three bottom-mounted ADCPs paired with temperature-

[4] Values are positive for flux out of the Arctic.

conductivity sensors to measure the full velocity profile in shelf waters, two on the Greenland side and one on the Baffin. There are temperature-conductivity sensors at five additional shallow sites. At some shelf sites (1 in 2004/2005, 2 in 2005/2006, 4 in 2006/2007) there is an additional temperature-conductivity sensor at roughly 25-m depth in a package (IceCAT) developed at APL-UW; because this sensor measures within the low salinity layer near the ice, at significant risk of damage, it relays its data to a recording module at the seabed. If the sensor is snagged by ice, a weak link in the mooring line fails, permitting loss of the sensor while protecting the data module for later recovery.

Seagliders complement the moored instruments by providing fields of temperature and salinity at appropriate spatial resolution, right up to the surface, year-round and without ongoing ship support. The highly resolved hydrography in combination with time series of velocity, salinity and temperature provides a detailed picture of spatial and temporal variation. Such information is essential for the accurate estimation of fluxes and of their empirical uncertainty. Such measurements are already practical in the absence of pack ice. Present effort is focussed on developing acoustic navigation and communication to provide the same capability when when ice prevents surfacing.

Imagery-based ice-feature tracking is used to augment ice velocity measurements collected by the upward-looking ADCPs.

Although this is a respectable array with instruments at 14 sites and with current measured at 9, the average site spacing of 40 km is still far greater than the decorrelation scale of ocean variability (Melling et al., 2001; Tang et al., 2004). This is apparent when considering how data from individual moorings contribute to the 2-Sv volume flux for 2004-05 (Figure 29). The plotted time series are the area-weighted contributions to the volume flux, each based on data from a single mooring. The time series are obviously poorly correlated with the result that there are long-lived and spurious fluctuations in the estimated flux. The accurate point measurements clearly require the complementary data from Seagliders to resolve variability within the Strait and thereby provide the hydrographic detail needed for intelligent interpolation between time series at fixed locations.

8.10 Summary and outlook

The tabulation (Table 6) of volume and fresh-water fluxes through the gateways for Pacific Arctic through-flow is the outcome of our work in its most concise form.

All of the ASOF initiatives in the North American Arctic are clearly works in progress. Our research is advancing steadily along learning curves in measurement, in interpretation of observations and in modeling. Our confidence to integrate with other ASOF sub-programmes and to explore the impact of global change is growing. Nonetheless, manifest environmental, logistical and technical complexity makes Pacific Arctic through-flow a big topic for research.

The following are brief assessments of progress towards desired outcomes.

Quantitative knowledge of flux magnitude & variability:

We continue to benefit from promising new observational tools – ADCP, ice-profiling sonar, ICYCLER, IceCat, Sea Glider, methods for direction reference – and developing numerical models. We have derived new values for fluxes, but values are less forthcoming for fresh-water than for volume. The bias and uncertainty of flux estimates are poorly known. Time series are far shorter than a decade in most instances and are non-existent for fresh-water at some key gateways. In consequence, the temporal overlap of time series within the North American Arctic is not yet sufficient to balance the budgets of Arctic seawater or freshwater.

Forcing and controls on Pacific Arctic through-flow:

Researchers favour the steric anomaly of the North Pacific as the prime mover of Pacific Arctic through-flow, but renewed effort to define the magnitude and temporal variation of this anomaly would be beneficial. Wind may augment or oppose steric forcing. There has been significant recent advance in the understanding of wind amplification in sea straits via mesoscale atmospheric effects and of its consequences for Pacific Arctic through-flow.

Models and observations agree that baroclinicity is an important attribute of Pacific Arctic through-flow. In baroclinic flows the width of low-density boundary currents is comparable to the internal Rossby scale (here about 10 km: Leblond, 1980). With this constraint, wider channels cannot necessarily carry larger fluxes. We note that the flux through Lancaster Sound, nearly 70 km wide, is only three times that through Cardigan Strait which has one ninth the width.

Numerical simulation has demonstrated that flow through Nares Strait is strongly influenced by atmospheric forcing that has been amplified by local orography via mesoscale atmospheric dynamics. Measurements of wind and temperature are needed in the planetary boundary layer to evaluate the simulations and to promote the understanding of oceanic and pack-ice responses. Because these processes may be important to through-flow in other areas, there is need for modelling at high resolution over a widened geographic domain.

Oceanic flows through the Pacific-Arctic gateways are thought to be controlled by friction and perhaps by rotational hydraulic effects. Numerical simulation of circulation within the Canadian Archipelago using a simple parameterization of drag has illustrated the importance of tidal current as a source of turbulence kinetic energy and therefore of resistance to flow at sub-tidal frequency. Since details are poorly developed, a future focus on these mechanisms in the context of Pacific Arctic through-flow is recommended.

Sea ice, as pack ice or as fast ice, covers the North American Arctic for much of the year. The impact of ice on channel flow is highly non-linear. It can range from an enhancement of wind forcing in the presence of rough mobile pack ice to a complete isolation from wind forcing by fast ice. In the latter instance, the immobile ice sheet exerts additional drag on oceanic flow. We recommend an initiative to understand the intermittent flow and blockage of sea ice in straits, with the ultimate objective of a reliable predictive capability.

Theory and simulation of through-flow:

There are many relevant theoretical topics to be addressed, ranging from the practical representation of rotational stratified flow in tidal channels to ocean hydrography and the circulation of freshwater and sea ice on a hemispheric scale. In particular, we need a clearer notion of the hydrologic asymmetry between the Atlantic and Pacific that creates the steric anomaly that may drive the Pacific Arctic through-flow. An improved theoretical understanding will contribute to the numerical models that must ultimately provide our capability to hind-cast and predict Pacific Arctic through-flow, and to generate spatially complete and temporally continuous perspectives that are inaccessible via direct measurement.

Response to global change:

The Pacific Arctic through-flow apparently responds to atmospheric and hydrologic forcing on a hemispheric scale. Our understanding of this forcing, of the varying storage of fresh-water within the Arctic Ocean and its ice cover and of the controls on out-flows to the Labrador Sea is not sufficient at present to support plausible hypotheses regarding the impact of changing climate on Pacific Arctic through-flow over the next century.

The practical task of ocean-flux measurement could benefit from continued focus on several issues:

There is need for a proven and agreed methodology for ocean-flux estimation. Table 7 summarizes the arrays presently installed in various gateways to measure Pacific Arctic through-flow. With two exceptions, the arrays fail to resolve the flow at the baroclinic Rossby scale (10 km) and all fail to measure salinity in the upper 30 m, where a large fraction of the fresh-water flux occurs (Melling, 2000). Two arrays do use a prototype instrument to sample the upper layer, but at too few locations. Table 7 joins discussion earlier in the chapter to illustrate that we have yet to justify our methodology for flux measurement. Arrays with improved resolution of flow structure across sections and improved delineation of shallow salinity structure can assist in this task. The data that we acquire with improved arrays may ultimately provide the justification for the simplifying assumptions that are now being made, a priori.

One component of a proven methodology is an error model for ocean-flux estimation. Expanded arrays will provide the redundancy required to advance our understanding of sampling error and observational bias. At present we lack the ancillary data to understand differences in computed fluxes on adjacent sections and cannot check the consistency of our results via independent means.

An integrated approach to the fresh-water fluxes moved as sea ice and as low salinity seawater is strongly advised. Fresh-water cycles between the seawater and ice phases with downstream movement and with the annual freeze-thaw cycle. At times the ice and ocean may transport fresh-water in opposite directions. Ice measurements lag those in the ocean except in the aspect of geographic coverage; otherwise, ice velocity is only coarsely resolved in time (3 days) and ice thickness is rarely measured.

The Arctic Sub-Arctic Ocean Fluxes study has recommended a decade of synoptic observation. We have been late starting in the west and the only time series to achieve the 10-year target is that in Bering Strait (Figure 30). The period of synoptic observation is 3 years (2003-06). A prolongation of existing time series is necessary to meet the original ASOF target.

At present we work hard to determine fresh-water flux, perhaps resolved as weekly or monthly averages. However, the ultimate impact of fresh-water in the receiving basins is critically dependent on the form in which it is delivered; the effect of a large seawater flux at salinity near 34.8 is very different from that of a small flux at near zero salinity, such as melting sea ice. In many cases we actually have the data in hand to report histograms of fresh-water flux according to salinity (Melling, 2000) – the separate reporting of ice and seawater contribution is a first step. Continuing diligence is to be encouraged.

We are beginning to exploit the potential of trace chemical and isotope anomalies to reveal the sources of fresh-water, decadal variability and the time scales of transit. The reward of this work will increase with the number of repeated geochemical surveys. With caution we can use some of the earlier (1985-1995) data, but sampling and analyses to modern standards have been completed only three times during the last decade. At this repetition interval, rapid change in some components of the ice-ocean system is already aliased. Continued regional surveys, at annual intervals in certain areas, and efforts to resolve the strong seasonal cycles in fresh-water components, are needed to move understanding forward at this time.

There is continuing need for new observational technology. Preliminary work with sea-level signals (via pressure recorders and satellite altimetry) shows promise and should be pursued more intensely, in conjunction with programmes of in situ observation. The challenge of measuring fresh-water flux within the top 30 m remains with us – new technological approaches are always welcome. Above all, there is a strong incentive for new instruments and methods that provide needed data at reduced cost.

Ocean circulation models of the Canadian Archipelago are afflicted by shortage in three domains, bathymetry, hydrography and surface meteorology. The first, required to build a realistic geometry for the Canadian polar shelf, is plentiful in some areas, but patchy or non-existent in others. In some areas the need could be addressed by facilitating the migration of existing survey data into an accessible digital archive; in other areas new surveys are required that meet the reasonable needs of numerical simulation – needs that are much more modest than those of navigation. A modest objective for hydrographic information is the acquisition of temperature-salinity data sufficient to prepare a synoptic picture for the entire Canadian polar shelf for each season of the year. From meteorology, we need ocean-relevant observations of surface wind and temperature, to evaluate mesoscale atmospheric models and to promote understanding of the seasonal cycle of sea-ice growth, consolidation, break-up and decay in the largest fast-ice domain in the world.

Acknowledgements

To be provided if appropriate

References

Aagaard, K. and E.C. Carmack. 1989. The role of sea ice and other fresh-water in the Arctic circulation. Journal of Geophysical Research 94, 14485-14498.

Aagaard, K. and P. Greisman. 1975. Towards new mass and heat budgets for the Arctic Ocean. Journal of Geophysical Research 80, 3821-3827.

Agnew, T.A. 1998. Drainage of multi-year sea ice from the Lincoln Sea. CMOS Bulletin 26(4), 101-103.

Agnew, T.A., B. Alt, R. De Abreu and S. Jeffers. 2001. The loss of decades old sea ice plugs in the Canadian Arctic Islands. In, Proceedings of the 6th Conference on Polar Meteorology and Oceanography, San Diego CA. American Meteorological Society (AMS) Boston.

Agnew, T. A., H. Le, and T. Hirose. 1997. Estimation of large scale sea ice motion from SSM/I 85.5 GHz imagery. Annals of Glaciology 25, 305-311.

Agnew, T.A. and J. Vandeweghe. 2005. Report on estimating sea-ice transport into the North Atlantic using the Advanced Microwave Scanning Radiometer (AMSR-E). Unpublished report, 21 pp.

Agnew, T.A., J. Vandeweghe and A. Lambe. 2006. Estimating the sea-ice-area flux across the Canadian Arctic Archipelago using the Advanced Microwave Scanning Radiometer (AMSR-E). Unpublished report, 20 pp.

Ahlnäs, K., and G.R. Garrison. 1984. Satellite and oceanographic observations of the warm coastal current in the Chukchi Sea. Arctic 37, 244-254.

Alkire, M.B., K.K. Falkner, I. Rigor, M. Steele and J. Morison. 2006. The return of Pacific waters to the upper layers of the central Arctic Ocean. Deep-Sea Research, submitted.

Amon, R.M.W., G. Budéus and B. Meon. 2003. Dissolved organic carbon distribution and origin in the Nordic Seas: Exchanges with the Arctic Ocean and the North Atlantic. Journal of Geophysical Research 108, doi:10.1029/2002JC001594.

Bacon, S., S., G. Reverdin, I.G. Rigor and H.M. Snaith. 2002. A freshwater jet on the east Greenland shelf. Journal of Geophysical Research 107, doi:10.1029/2001JC000935.

Barber, F.G. 1965. Current observations in Fury and Hecla Strait. Journal of the Fisheries Research Board of Canada 22, 225–229.

Bromwich, D.H., J.J. Cassano, T. Klein, G. Heinemann, K.M. Hines, K. Steffen and J.E. Box. 2001. Mesoscale modeling of katabatic winds over Greenland with the Polar MM5. Monthly Weather Review 129, 2290-2309.

Cassano, J.J., J.E. Box, D.H. Bromwich, L. Li and K. Steffen. 2001: Evaluation of Polar MM5 simulations of Greenland's atmospheric circulation. Journal of Geophysical Research 106, 33867-33890.

Cherniawsky, J.Y., W.R. Crawford, O.P. Nikitin and E.C. Carmack. 2005. Bering Strait transports from satellite altimetry, Journal of Marine Research 63, 887-900.

Clement, J.L., W. Maslowski, L.W. Cooper, J.M. Grebmeier and W. Walczowski. 2005. Ocean circulation and exchanges through the northern Bering Sea – 1979-2001 model results, Deep-Sea Research II 52, 3509-3540, doi:10.1016/j.dsr2.2005.09.010.

Coachman, L.K. and K. Aagaard. 1966. On the water exchange through Bering Strait. Limnology and Oceanography 11, 44-59.

Coachman, L.K. and K. Aagaard. 1981. Re-evaluation of water transports in the vicinity of Bering Strait. In, The Eastern Bering Sea Shelf: Oceanography and Resources Volume 1, (D. W. Hood & J. A. Calder, editors). National Oceanic and Atmospheric Administration Washington DC. 95-110.

Coachman, L.K., K. Aagaard and R.B. Tripp. 1975. Bering Strait: The Regional Physical Oceanography. University of Washington Press Seattle WA.

Codispoti, L.A. and D. Lowman. 1973. A reactive silicate budget for the Arctic Ocean. Limnology and Oceanography 18, 448-456.

Cooper, L.W., T.E. Whitledge, J.M. Grebmeier and T. Weingartner. 1997. The nutrient, salinity, and stable oxygen isotope composition of Bering and Chukchi Seas waters in and near Bering Strait. Journal of Geophysical Research 102, 12563-12573.

Cuny, J., P.B. Rhines and R. Kwok. 2005. Davis Strait volume freshwater and heat fluxes. Deep-Sea Research I 52, 519–542.

de Lange Boom, B.R., H. Melling and R.A. Lake. 1987. Late Winter Hydrography of the Northwest Passage: 1982, 1983 and 1984. Canadian Technical Report of Hydrography and Ocean Sciences No. 79, 165 pp. Unpublished report available from Institute of Ocean Sciences Box 6000 Sidney Canada V8L 4B2.

Deutsch, C., N. Gruber, Key, R.M., J.L. Sarmiento and A. Ganachaud. 2001. De-nitrification and N_2 fixation in the Pacific Ocean. Global Biogeochemical Cycles 15, 483-506. doi:10.1029/2000GB001291.

Dunphy, M., F. Dupont, C.G. Hannah and D. Greenberg. 2005. Validation of Modeling System for Tides in the Canadian Arctic Archipelago. Canadian Technical Report of Hydrography and Ocean Sciences 243, vi + 70 pp. Unpublished report available from Bedford Institute of Oceanography Box 1006 Dartmouth Canada B2Y 4A2.

Ekwurzel, B., P. Schlosser, R.A. Mortlock and R.G. Fairbanks. 2001. River runoff, sea ice meltwater, and Pacific water distribution and mean residence times in the Arctic Ocean. Journal of Geophysical Research 106, 9075-9092.

Falkner, K.K., M.C. O'Brien, H. Melling, E. C. Carmack, F. A. McLaughlin, A. Münchow and E. P. Jones. 2006. Interannual variability of dissolved nutrients in the Canadian Archipelago and Baffin Bay with implications for fresh-water flux. Journal of Geophysical Research Bio-Geosciences, submitted.

Fissel, D.B., J.R. Birch, H. Melling and R.A. Lake. 1988. Non-tidal Flows in the Northwest Passage. Canadian Technical Report of Hydrography and Ocean Sciences No. 98, 143 pp. Unpublished report available from Institute of Ocean Sciences Box 6000 Sidney Canada V8L 4B2

Gruber, N., and J.L. Sarmiento. 1997. Global patterns of marine nitrogen fixation and de-nitrification. Global Biogeochemical Cycles 11, 235-266.

Guo, Z., D.H. Bromwich and J.J. Cassano. 2003: Evaluation of Polar MM5 simulations of Antarctic atmospheric circulation. Monthly Weather Review 131, 384-411.

Häkkinen, S. and A. Proshutinsky. 2004. Fresh-water content variability in the Arctic Ocean. Journal of Geophysical Research 109, doi:10.1029/2003JC001940.

Holloway, G. and T. Sou. 2002. Has Arctic sea ice rapidly thinned? Journal of Climate 15, 1691-1701.

Jones, E.P. and L.G. Anderson. 1990. On the origin of the properties of the Arctic Ocean halocline north of Ellesmere island: results from the Canadian Ice Island, Continental Shelf Research 10, 485-498.

Jones, E.P. and L.G. Anderson. 2007. Is the global conveyor belt threatened by the Arctic Ocean fresh-water outflow?, in ASOF Book, edited by D. e. al.

Jones, E.P., L.G. Anderson and J.H. Swift. 1998. Distribution of Atlantic and Pacific waters in the upper Arctic Ocean: Implications for circulation. Geophysical Research Letters 25, 765-768.

Jones, E.P. and A.R. Coote. 1980. Nutrient distributions in the Canadian Archipelago: Indicators of summer water mass and flow characteristics. Canadian Journal of Fisheries and Aquatic Science 37, 589-599.

Jones, E.P., J.H. Swift, L.G. Anderson, M. Lipizer, G. Civitarese, K.K. Falkner, G. Kattner and F.A. McLaughlin. 2003. Tracing Pacific water in the North Atlantic Ocean. Journal of Geophysical Research 108, doi:10.1029/2001JC001141.

Kinney, P., M.E. Arhelger and D.C. Burrell. 1970. Chemical characteristics of water masses in the Amerasian Basin of the Arctic Ocean. Journal of Geophysical Research 75, 4097-4104.

Kliem, N. and D. A. Greenberg. 2003. Diagnostic simulations of the summer circulation in the Canadian Arctic Archipelago. Atmosphere-Ocean 41, 273–289.

Kwok, R. 2005. Variability of Nares Strait ice flux, Geophysical Research Letters 32, L24502, doi:10.1029/2005GL024768

Kwok, R. 2006. Exchange of sea ice between the Arctic Ocean and the Canadian Arctic Archipelago. Geophysical Research Letters 33, L16501, doi:10.1029/2006GL027094.

Kwok, R., G.F. Cunningham and S. Yueh. 1999. Area Balance of Arctic Ocean Perennial Ice Zone: October 1996 - April 1997. Journal of Geophysical Research 104, 25747. doi:10.1029/1999JC900234.

Kwok, R., A. Schweiger, D. A. Rothrock, S. Pang, and C. Kottmeier. 1998. Sea ice motion from satellite passive microwave imagery assessed with ERS SAR and buoy motions. Journal of Geophysical Research 103, 8191-8214.

Lammers, R.B., A.I. Shiklomanov, C.J. Vorosmarty, B.M. Fekete and B.J. Peterson. 2001. Assessment of contemporary Arctic river runoff based on observational discharge records, Journal of Geophysical Research 106, 3321-3334.

LeBlond, P.H. 1980. On the surface circulation in some channels of the Canadian Arctic Archipelago. Arctic 33, 189-197.

Loder, J.W., B. Petrie and G. Gawarkiewicz. 1998. The coastal ocean off north-eastern North America: A large-scale view. Chapter 5 in The Sea Volume 11, John Wiley & Sons Inc. 105-133.

Maslowski, W., J.L. Clement and W. Walczowski. 2003. Modeled Arctic sub-Arctic ocean fluxes during 1979-2001. Abstract #9554, EGS-AGU-EUG Joint Assembly, Nice France, 6-11 April 2003.

McLaren, A.S., P. Wadhams and R. Weintraub. 1984. The sea ice topography of M'Clure Strait in winter and summer of 1960 from submarine profiles. Arctic 37, 110-120.

Melling, H. 2000. Exchanges of fresh-water through the shallow straits of the North American Arctic. In, The Fresh-water Budget of the Arctic Ocean. Proceedings of a NATO Advanced Research Workshop, Tallinn Estonia, 27 April – 1 May 1998, E.L. Lewis et al. (editors). Kluwer Academic Publishers Dordrecht Netherlands, 479-502.

Melling, H. 2002. Sea ice of the northern Canadian Archipelago. Journal of Geophysical Research 107, 3181, doi:10.1029/2001JC001102.

Melling, H., Y. Gratton and R.G. Ingram. 2001. Ocean circulation within the North Water polynya of Baffin Bay. Atmosphere-Ocean 39, 301-325.

Melling, H., P.H. Johnston and D.A. Riedel. 1995. Measurement of the topography of sea ice by moored sub-sea sonar. Journal of Atmospheric and Oceanic Technology 12, 589-602.

Melling, H., R.A. Lake, D.R. Topham and D.B. Fissel. 1984. Oceanic thermal structure in the western Canadian Arctic. Continental Shelf Research 3, 233-258.

Melling, H. and D.A. Riedel. 1996. Development of seasonal pack ice in the Beaufort Sea during the winter of 1991-92: A view from below. Journal of Geophysical Research 101, 11975-11992.

Mosby, H. 1962. Water, salt and heat balance of the North Polar Sea and of the Norwegian Sea. Geophysica Norvegica 24, 289-313.

Muench, R.D. 1971. The physical oceanography of the Northern Baffin Bay Region. AINA Research Paper No. 1. The Arctic Institute of North America, University of Calgary, Calgary AB Canada. 150 pp.

Münchow, A., H. Melling and K.K. Falkner. 2005. An observational estimate of volume and freshwater flux leaving the Arctic Ocean through Nares Strait. Journal of Physical Oceanography 36, 2025-2041.

Östlund, H.G., and G. Hut. 1984. Arctic Ocean water mass balance from isotope data. Journal of Geophysical Research 89, 6373-6381.

Padman, L. and S. Erofeeva. 2004. A barotropic inverse tidal model for the Arctic Ocean. Geophysical Research Letters 31, L02303, doi:10.1029/2003GL019003.

Paquette, R.G. and R. H. Bourke. 1974. Observations on the coastal current of Arctic Alaska. Journal of Marine Research 32, 195-207.

Prinsenberg, S.J. 1988. Damping and phase advance of the tide in western Hudson Bay by the annual ice-cover. Journal of Physical Oceanography 18, 1744-1751.

Prinsenberg, S.J. and E.B. Bennett. 1987. Mixing and transports in Barrow Strait, the central part of the Northwest Passage. Continental Shelf Research 7, 913-935.

Prinsenberg, S.J. and E.B. Bennett. 1989. Vertical variations of tidal currents in shallow land fast ice-covered regions. Journal of Physical Oceanography 19, 1268-1278.

Prinsenberg, S.J. and J. Hamilton. 2005. Monitoring the volume, freshwater and heat fluxes passing through Lancaster Sound in the Canadian Arctic Archipelago. Atmosphere-Ocean 43, 1-22.

Pritchard, R.S., R.W. Reimer and M.D. Coon. 1979. Ice flow through straits. In Proceedings of POAC'79 Volume 3, Norwegian Institute of Technology Trondheim Norway. 61-74.

Proshutinsky, A.Y., and M. A. Johnson. 1997. Two circulation regimes of the wind-driven Arctic Ocean. Journal of Geophysical Research 102, 12,493-412,514.

Roach, A.T., K. Aagaard, C.H. Pease, S.A. Salo, T. Weingartner, V. Pavlov and M. Kulakov. 1995. Direct measurements of transport and water properties through the Bering Strait. Journal of Geophysical Research 100, 18443-18457.

Roff, J.C., and L. Legendre. 1986. Physico-chemical and biological oceanography of Hudson Bay. In, Canadian Inland Seas, I. P. Martini (editor), Elsevier New York. 265-291.

Ross, C. 1992. Moored current meter measurements across Davis Strait. NAFO Research Document 92/70.

Sadler, H.E. 1976. Water heat and salt transports through Nares Strait Ellesmere Island. Journal of the Fisheries Research Board of Canada 33, 2286-2295.

Sadler, H.E. 1982. Water flow into Foxe Basin through Fury and Hecla Strait. Le Naturaliste Canadian 109, 701-707.

Samelson, R.M. and S.J. Lentz, 1994. The horizontal momentum balance in the marine atmospheric boundary layer during CODE-2. Journal of the Atmospheric Sciences 51, 3745-3757.

Samelson, R.M., T. Agnew, H. Melling and A. Münchow. 2006. Evidence for atmospheric control of sea-ice motion through Nares Strait. Geophysical Research Letters 33, L02506, doi:10.1029/2005GL025016.

Sanderson, B.G. 1987. Statistical properties of iceberg motion at the western entrance of Lancaster Sound. In Proceedings of Oceans'87. MTS/IEEE Volume 19, 17-23.

Schlosser, P., B. Ekwurzel, S. Khatiwala, B. Newton, W. Maslowski and S. Pfirman. 2000. Tracer studies of the Arctic fresh-water budget. In, The Fresh-water Budget of the Arctic Ocean. E.L. Lewis (editor), Kluwer Academic, Dordrecht. 453-478.

Serreze, M.C., A.P. Barrett, A.G. Slater, R.A. Woodgate, K. Aagaard, R. Lammers, M. Steele, R. Moritz, M. Meredith and C.M. Lee (submitted). The large-scale fresh-water cycle of the Arctic. Journal of Geophysical Research, submitted.

Smith, J.N., K.M. Ellis and T Boyd. 1999. Circulation features in the Central Arctic Ocean revealed by nuclear fuel reprocessing tracers from SCICEX 95 and 96. Journal of Geophysical Research 104, 29633-29677.

Sodhi D.S. 1977. Ice arching and the drift of pack ice through restricted channels. CRREL Report No 77-18, U.S. Army Cold Regions Research and Engineering Laboratory, Hanover, N.H. Available NTIS. 11 pp.

Steele, M., D. Thomas, D. Rothrock and S. Martin. 1996. A simple model of the Arctic Ocean fresh-water balance 1979-1985. Journal of Geophysical Research 101, 20833-20848.

Stigebrandt, A. 1984. The North Pacific: a global-scale estuary. Journal of Physical Oceanography 14, 464-470.

Strain, P.M., and F.C. Tan. 1993. Seasonal evolution of oxygen isotope-salinity relationships in high-latitude surface waters. Journal of Geophysical Research 98, 14,589-514,598.

Tang, C.L., C.K. Ross, T. Yao, B. Petrie, B.M. DeTracy and E. Dunlop. 2004. The circulation water masses and sea ice of Baffin Bay. Progress in Oceanography 63, 183-228

Taylor, J.R., K.K. Falkner, U Schauer and M. Meredith 2003. Quantitative considerations of dissolved barium as a tracer in the Arctic Ocean. Journal of Geophysical Research 108, doi:10.1029/2002JC001635.

Tremblay, J.-É., Y. Gratton, E.C. Carmack, C.D. Payne and N.M. Price. 2002. Impact of the large-scale Arctic circulation and the North Water polynya on nutrient inventories in Baffin Bay. Journal of Geophysical Research 107, doi:10.1029/2000JC000595.

Weingartner, T.J., S.L. Danielson and T.C. Royer. 2005. Fresh-water variability and predictability in the Alaska Coastal Current. Deep-Sea Research II 52, 169-191. doi:110.1016/j.dsr1012.2004.1009.1030.

Wijffels, S.E., R.W. Schmitt, H.L. Bryden and A. Stigebrandt. 1992. Transport of freshwater by the oceans. Journal of Physical Oceanography 22, 155-162.

Williams, C. E., W. Maslowski, J.C. Clement and A.J. Semtner. 2004. Fresh-water Fluxes from the Arctic into the North Atlantic Ocean: 1979-2002 model results. American Geophysical Union Fall Meeting 2004, 2004AGUFM.C54A-05W.

Winant, C.D., C.E. Dorman, C.A. Friehe and R.C. Beardsley. 1988. The marine layer off northern California: An example of supercritical channel flow. Journal of Atmospheric Sciences 45, 3588-3605.

Woodgate, R.A. and K. Aagaard. 2005. Revising the Bering Strait fresh-water flux into the Arctic Ocean. Geophysical Research Letters 32, L02602. doi:10.1029/2004GL021747.

Woodgate, R.A., K. Aagaard and T.J. Weingartner. 2005a. Monthly temperature, salinity, and transport variability of the Bering Strait through-flow. Geophysical Research Letters 32, L04601. doi:10.1029/2004GL021880.

Woodgate, R.A., K. Aagaard and T.J. Weingartner. 2005b. A year in the physical oceanography of the Chukchi Sea: Moored measurements from autumn 1990-1991, Deep-Sea Research II 52, 3116-3149, 10.1016/j.dsr2.2005.10.016.

Woodgate, R.A., K. Aagaard and T.J. Weingartner. 2006. Inter-annual changes in the Bering Strait fluxes of volume, heat and fresh-water between 1991 and 2004. Geophysical Research Letters 33, L15609. doi:10.1029/2006GL026931.

Yamamoto-Kawai, M., N Tanaka and S. Pivovarov. 2005. Fresh-water and brine behaviors in the Arctic Ocean deduced from historical data of $\delta^{18}O$ and alkalinity (1929–2002). Journal of Geophysical Research 110, doi:10.1029/2004JC002793.

Yamamoto-Kawai, M., F.A. McLaughlin, E.C. Carmack, S. Nishino and K. Shimada. 2006. Fresh-water budget of the Canada Basin Arctic Ocean from geochemical tracer data. Journal of Geophysical Research, submitted.

List of Tables

Tables

Table 1. Fluxes of volume, fresh-water and heat through Lancaster Sound as seasonal and annual averages for August 1998 to August 2004. The reference salinity for fresh-water flux is 34.8 and the reference temperature for heat flux is -0.1ºC. Arctic exports have positive value. Heat-flux values in this table correct an error in Table 5 of Prinsenberg and Hamilton (2005), where the unit was stated as 10^5 W.

		Fall	Winter	Spring	Summer	Year
1998-1999	Volume, Sv	-0.01	0.37	0.48	0.70	0.39
	Fresh-water, mSv	**10**	**26**	**31**	**44**	**26**
	Heat, TW	-0.0	-2.2	-3.1	-4.2	-2.4
1999-2000	Volume, Sv	0.25	0.91	1.09	1.32	0.89
	Fresh-water, mSv	**20**	**56**	**65**	**81**	**56**
	Heat, TW	-1.4	-5.4	-6.9	-7.3	-5.3
2000-2001	Volume, Sv	0.97	0.82	0.81	1.19	0.95
	Fresh-water, mSv	**59**	**51**	**51**	**72**	**58**
	Heat, TW	-5.2	-5.4	-5.2	-6.4	-5.5
2001-2002	Volume, Sv	0.11	0.35	0.87	0.93	0.56
	Fresh-water, mSv	**14**	**22**	**55**	**70**	**40**
	Heat, TW	-0.8	-2.2	-5.2	-6.3	-3.3
2002-2003	Volume, Sv	0.60	0.54	1.18	1.13	0.86
	Fresh-water, mSv	**45**	**34**	**77**	**92**	**62**
	Heat, TW	-3.2	-3.4	-7.5	-6.3	-5.1
2003-2004	Volume, Sv	0.31	0.45	0.63	1.24	0.57
	Fresh-water, mSv	**35**	**34**	**43**	**93**	**45**
	Heat, TW	-2.0	-2.9	-3.4	-6.2	-3.2

Table 2. Model-simulated fluxes of volume, fresh water and heat through the Canadian Archipelago (after Kleim and Greenberg, 2003). The reference salinity for fresh-water flux is 34.8 and the reference temperature for heat flux is -0.1ºC. Arctic exports have positive value.

	Diagnostic			Barotropic
	Volume (Sv)	Fresh-water (mSv)	Heat (10^{12} W)	Volume (Sv)
Barrow Strait	0.3	20	-1.3	1.8
Jones Sound	0.2	10	-0.8	0.6
Nares Strait	0.4	20	-1.3	2.4
Total	0.9	50	-3.4	4.8

Table 3. Annual average areal flux of ice between the Arctic Ocean and the Canadian polar shelf during the last decade. The unit is 1000 km^2. Exports from the Arctic Ocean to the shelf have positive value.

	Amundsen Gulf	M'Clure Strait	QEI south	QEI north	Nares Strait
1996-2002 (Sep-Aug) [a]					33 ±13
1997-2002 (Sep-Aug) [b]	-85 ±26	-20 ±24	6 ±5	2 ±6	
2002-2006 (Sep-Jun) [c]	-14 ±19	-5 ±14	30 ±8	6 ±4	

[a] Kwok (2005)
[b] Kwok et al. (2006)
[c] Agnew et al. (2006)

Table 4. Annual average areal flux of ice between the Canadian polar shelf and Baffin Bay during the last decade. The unit is 1000 km^2. Arctic exports have positive value.

	Lancaster Sound	Jones Sound	Smith Sound	Baffin Bay	Davis Strait
1996-2002 (Oct-Apr) [a]			34 ±_		
2002-2004 (Oct-May) [b]				690 ±80	610 ±70
2002-2006 (Sep-Jun) [c]	48 ±6	10 ±3	9 ±2		

[a] Kwok et al. (1999)
[b] Agnew and Vandeweghe (2005)
[c] Agnew et al. (2006)

Table 5. Estimates of the net fluxes of volume and fresh-water through Davis Strait. Those for 2004-2006 in the lower part of the table are preliminary. Arctic exports have positive value.

Method	Data Source	Location	Includes shelves?	Year	Timing	Volume Flux (Sv)	Fresh-water Flux (mSv)
Geostrophy [a]	CTD section	66.25º N		1987	September	5.7	195
Geostrophy [a]	CTD section	66.25º N		1988	September	1.5	126
Geostrophy [a]	CTD section	66.25º N		1989	September	5.7	286
Currents & geostrophy [a]	Current meters	66.25º N		1987-1990	3-y mean	2.6	92
Currents & geostrophy [a]	Current meters	66.25º N	No	1987-1990	3-y mean	3.4	130
Currents & geostrophy [b]	Current meters	66.25º N	No	1987-1990	3-y mean	2.6	99
Currents & geostrophy [c]	Current meters	66.25º N	No	1987-1990	3-y mean	3.3	120
Currents & geostrophy [d]	Current meters	66.25º N	No	1987-1990	3-y mean	3.1	
1/12° simulation [e]	Ocean model			1979-2001	21-y mean		76
Geostrophy [f]	CTD section	Northern line		2004	September	2.5	130
Geostrophy [f]	CTD section	Mooring line		2004	September	3.1	110
Geostrophy [f]	CTD section	66.25º N		2004	September	2.0	98
Geostrophy [f]	CTD section	Southern line		2004	September	-0.3	34
Currents [f]	ADCP	Mooring line		2004-05	1-y mean	2.0	
Geostrophy [f]	CTD section	Northern line		2005	September	2.8	
Geostrophy [f]	CTD section	Mooring line		2005	September	2.8	
Geostrophy [f]	CTD section	66.25º N		2005	September	2.5	
Geostrophy [f]	CTD section	Southern line		2005	September	0.9	
Geostrophy [f]	Sea Glider CTD	Mooring line	No	2006	September		72
Geostrophy [f]	Sea Glider CTD	Mooring line	No	2006	September		102
Geostrophy [f]	Sea Glider CTD	Mooring line	No	2006	September		115

[a] Cuny et al. (2005)
[b] Tang et al. (2004)
[c] Loder et al. (1998)
[d] Ross (1992)
[e] Maslowski et al. (2003)
[f] APL-UW unpublished data

Table 6. Summary of fluxes through the gateways for Pacific Arctic through-flow, estimated as described in this chapter and subject to many cautions – buyer beware. The value is positive for Arctic out-flow.

	Seawater Volume (Sv)	Oceanic fresh-water (mSv)	Ice area (1000s km^2)	Fresh-water as ice [a] (mSv)
Bering Strait	-0.8	-82		
Amundsen Gulf			-53	-1.7 [1 m]
M'Clure Strait			-13	-0.8 [2 m]
Sverdrup Basin			20	2.5 [4 m]
Lancaster Sound	0.7	48	48	1.5 [1 m]
Cardigan Strait & Hell Gate	0.3		10	0.3 [1 m]
Nares Strait	0.8 [b]	25	33	4.2 [4 m]
Baffin Bay			690	22 [1 m]
Davis Strait [c]	2.0	100	610	19 [1 m]

[a] Ice thickness has been estimated
[b] Snap-shot in time
[c] Not including flux over the Greenland shelf

Table 7. Summary of the arrays now installed to measure fresh-water flux.

	Width of gateway (km)	Number of moorings (current)	Mooring separation (km)	Maximum depth (m)	Number of levels of salinity [a]	Top level of salinity (m)
Bering Strait	76	1-2	38-76	50	1	40
Lancaster Sound	68	2-4	17-34	280	1-3+	30 (5)[b]
Cardigan Strait, Hell Gate	12	2	6	180	1	100
Nares Strait	38	8	5	380	5	30
Davis Strait	360	9	40	1000	1-3+	50 (25)[b]

[a] '+' indicates more levels measured by prototype near-surface instrument.
[b] Shallow depth measured by prototype instrument at one site only.

List of Figures

Figure 16. Time series of current along Kennedy Channel near Ellesmere Island from August 2003-2006; tides have been removed. The most obvious variability occurs at periods typical of synoptic weather.

Figure 17. The irregular triangular grid currently used for numerical simulation of circulation over the Canadian polar shelf. There are 76,000 elements (triangles) and 44,000 nodes (computation points). The mean separation of nodes is 7.8 km; the minimum and maximum are 1.1 and 80 km. Kliem and Greenberg (2003) used 20,000 elements and 12,000 nodes with 2.3-83 km separation.

Figure 18. The tidal mixing factor h/u^3 (contours are logarithmically spaced). Two regions with the smallest values (strongest mixing) are expanded for detail. The upper inset is centred on Hell Gate, Cardigan Strait, Queens Channel and Penny Strait. The lower is the region around the Boothia Peninsula. (after Dunphy et al. 2005).

Figure 19. Surface elevation as a proxy for transport (Nicolai Kliem DMI personal communication and http://ocean.dmi.dk/staff/nk/ArcticArchipelago/ - 3D non-linear diagnostic).

Figure 20. Gateways for calculation of ice-area flux from sequential satellite images.

Figure 21. Average fields of sea-level pressure and vector wind for January 2005. These data from simulations using the MM5 clearly reveal meteorological features on both synoptic and meso scales.

Figure 22. Vectors in the panels on the upper right display the mean wind and stress and the principal EOFs of these variables plotted against grid number along the line marked on the adjacent map; grid number increases from south to north. The panels on the lower right display the eigenvalues plotted against month, beginning in August 2003.

Figure 23. Year-long series of along-channel surface wind in Nares Strait, calculated using the linear dependence of wind on the along-channel difference in sea-level pressure established by Samelson et al. (2006). Pressure was measured at Alert and on the Carey Islands.

Figure 24. Silicate versus salinity for seawater samples acquired in Smith Sound during August of several years. Added curves envelope data from 1977 and 2003 (solid lines) and from 1997 (dashed line). Within both envelopes, the concentration is highest on the western side of the straits, although in 1977 ice prevented sampling on the western side. Note the shift to more concentrated silica in 1997. Note also the high silica concentration (strong Pacific influence) in northern Nares Strait in 2003; these values from Robeson Channel are comparable to those measured 600 km to the south in Smith Sound in 1997 (Falkner et al., 2006).

Figure 25. Bathymetry of Davis Strait. The coloured underlay represents long-term mean sea-surface temperature. Square symbols mark the locations of moorings placed in September 2004 in a new initiative to measure oceanic fluxes. Open circles mark recent conventional hydrographic surveys. Vectors depict depth-averaged current from instruments on moorings in the 1980s.

Figure 26. Hydrographic section across Davis Strait measured in September 2004, showing temperature (ºC, left panel) and salinity (right panel). The station spacing was about 25 km.

Figure 27. Hydrographic structure within the deep trough of Davis Strait measured by Sea Glider at approximately 5-km resolution.

Figure 28. Schematic representation of the array of instruments to measure fresh-water flux through Davis Strait.

Figure 29. Time series of area-weighted contributions to volume flux through Davis Strait, based on data from individual moorings during September 2004-2005.

Figure 30. Lifetimes of moored arrays within the gateways for Pacific-Arctic through-flow. The bars span those years during which current was measured for much of the time, but perhaps not in sufficient detail to permit the calculation of fluxes.

Figures

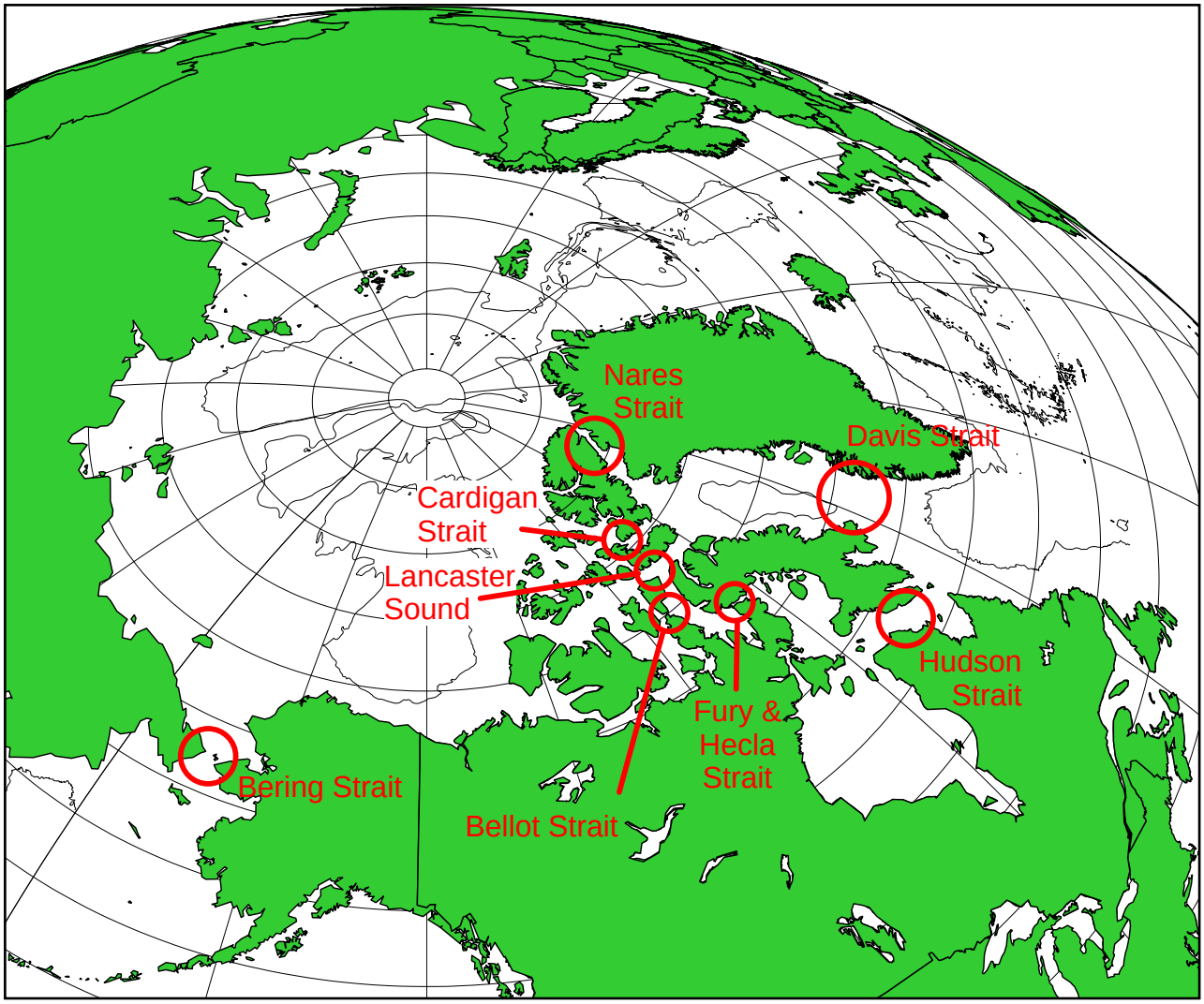

Figure 1. The Arctic Ocean with focus on the North American shelves. The gateways for Pacific Arctic through-flow are indicated. To reduce congestion, the Lancaster Sound tag has been used as a single identifier of Barrow Strait to the west and Wellington Channel to the north-west and the Cardigan Strait tag also represents nearby Hell Gate. The 1000-m isobath is plotted to delineate the continental shelves, ridges and ocean basins.

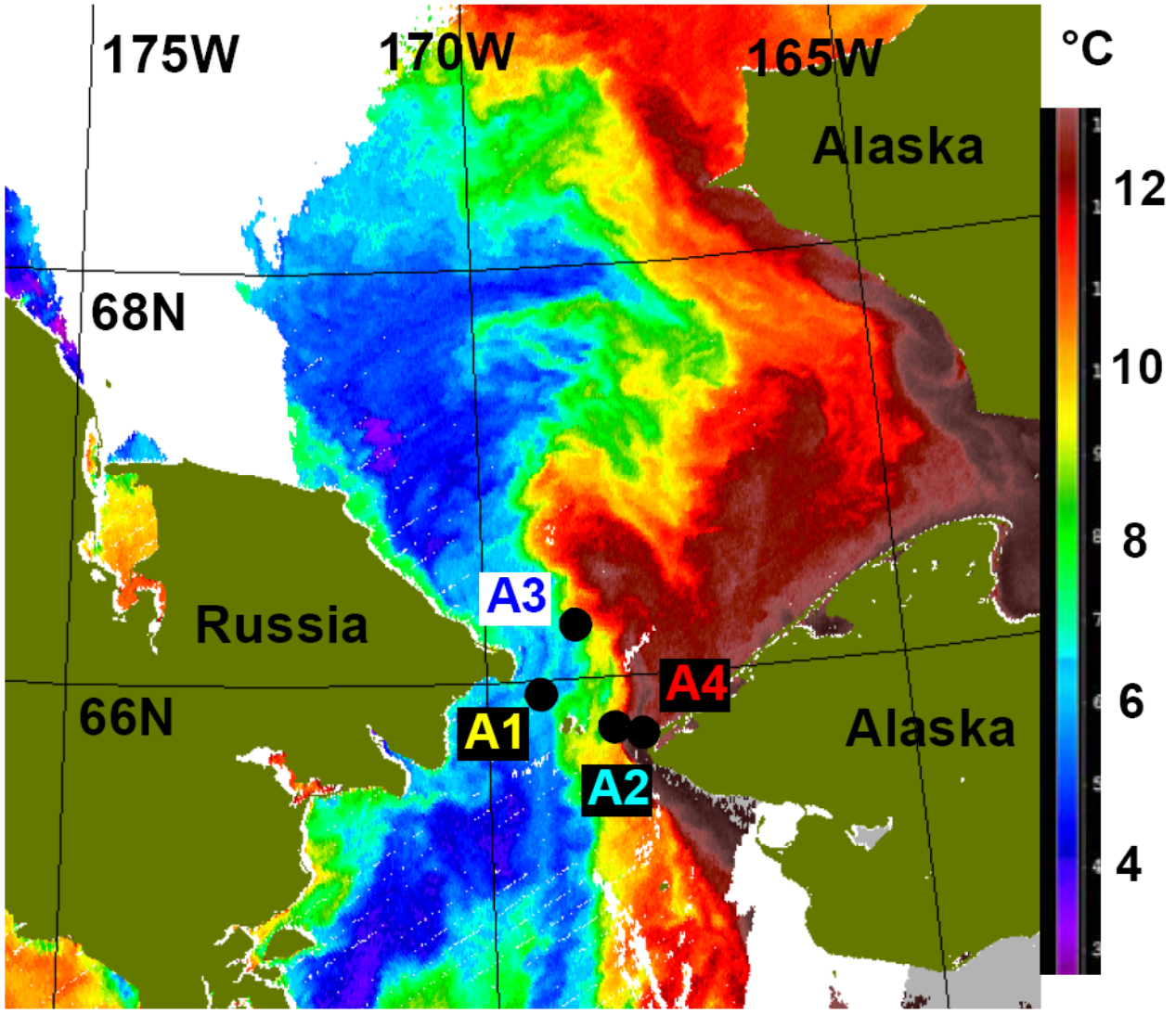

Figure 2. Bering Strait showing the locations of moorings for determining through-flow (dots). The background is a Modis/Aqua level 1 image displaying sea-surface temperature on 26 August 2004 (courtesy NASA/Goddard Space Flight Center). White areas are obscured by clouds.

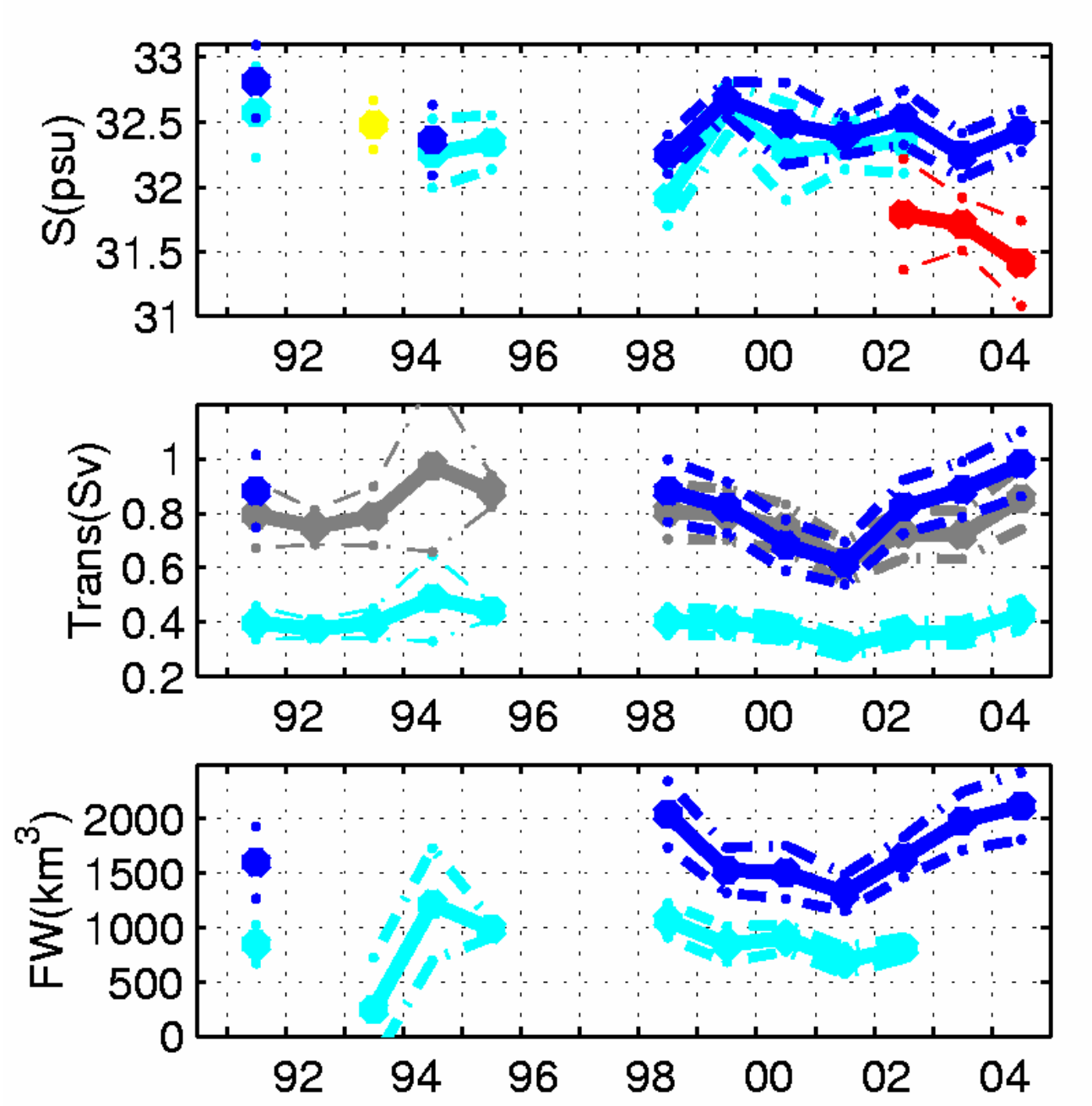

Figure 3. Annual mean values of near-bottom salinity (S), volume flux (Trans) and fresh-water flux (FW) derived from Bering Strait moorings as follows (A1: yellow, A2: cyan, A3: blue, A4: red). For flux estimates, blue (from A3) represents the entire strait and cyan (from A2) only the eastern channel. For transport, the grey line represents the entire strait, estimated from A2 only. Dashed lines indicate uncertainty in the means.

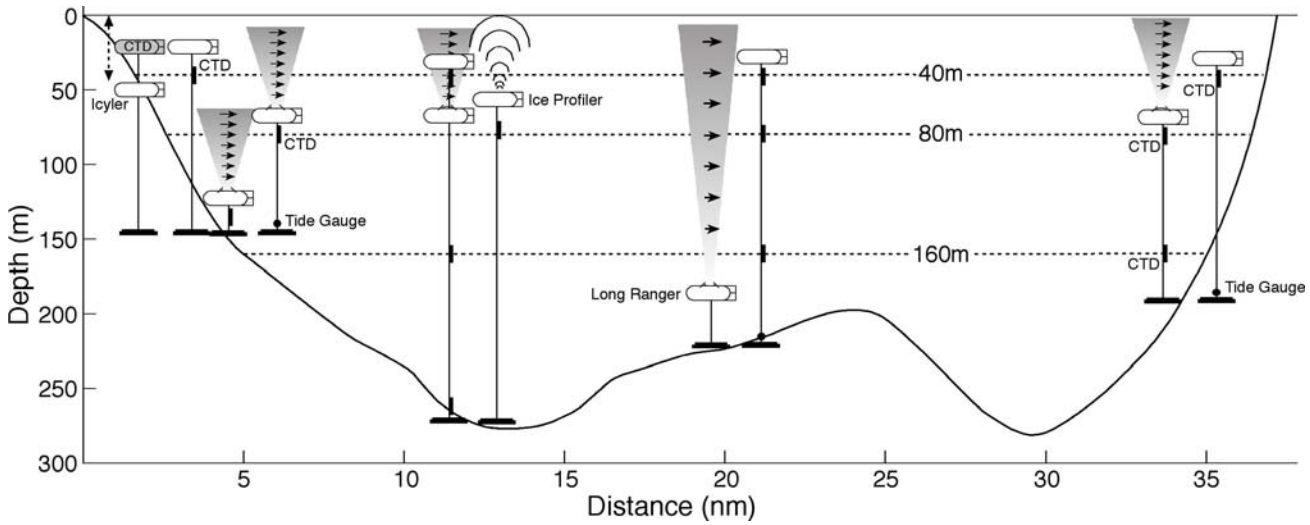

Figure 4. The expanded array of moorings in Lancaster Sound used for through-flow measurements during 2005-2006. The instruments have been concentrated near the southern shore (left of figure) in order to detect the buoyancy boundary current which carries much of the Arctic through-flow.

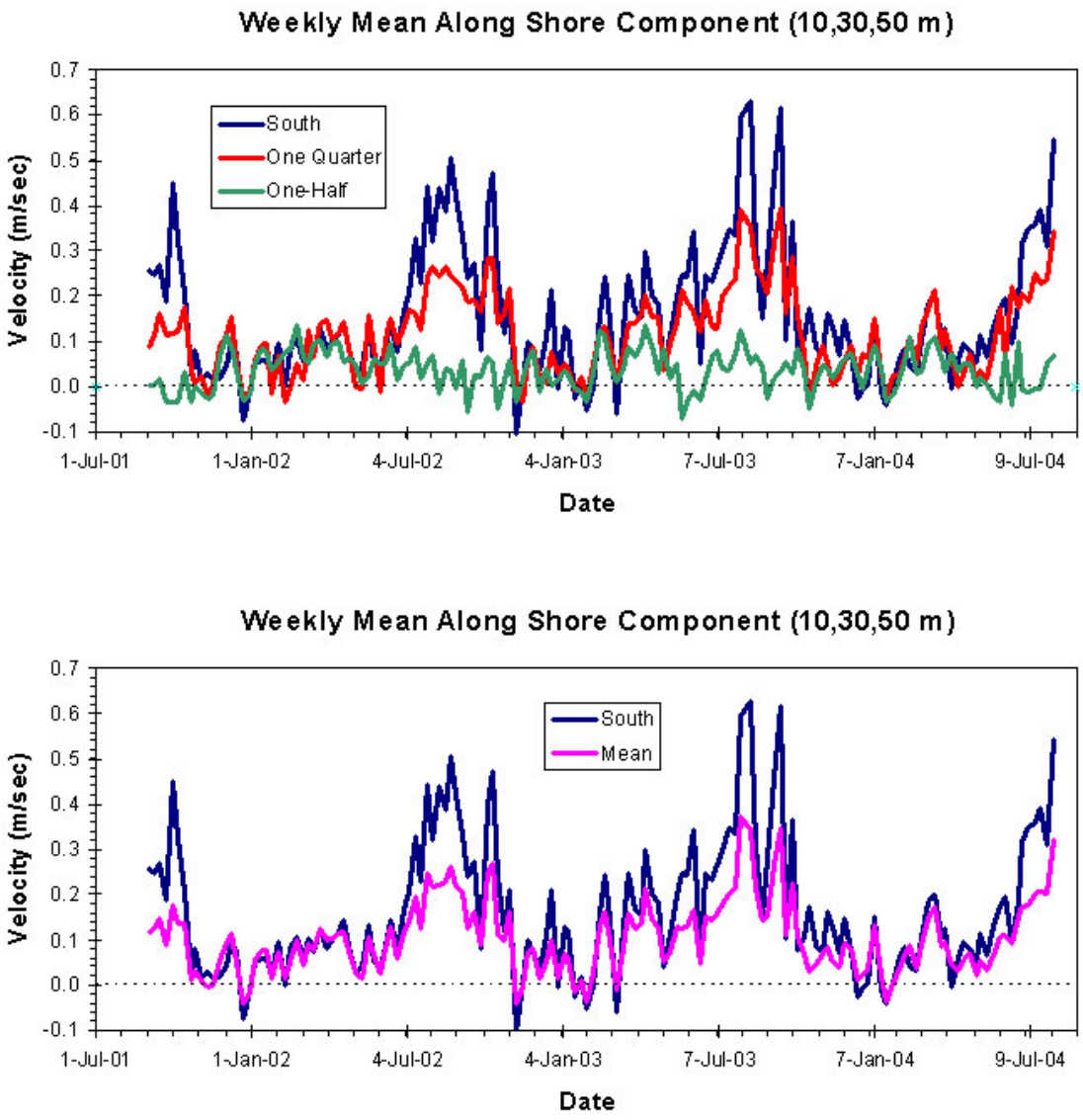

Figure 5. Weekly averaged values of surface current computed from the mean of measured flows at 10, 30 and 50 m for 3 locations in the southern half of Lancaster Sound (upper panel). Average of the weekly data from the 3 locations compared to the weekly data from the southernmost site (lower panel).

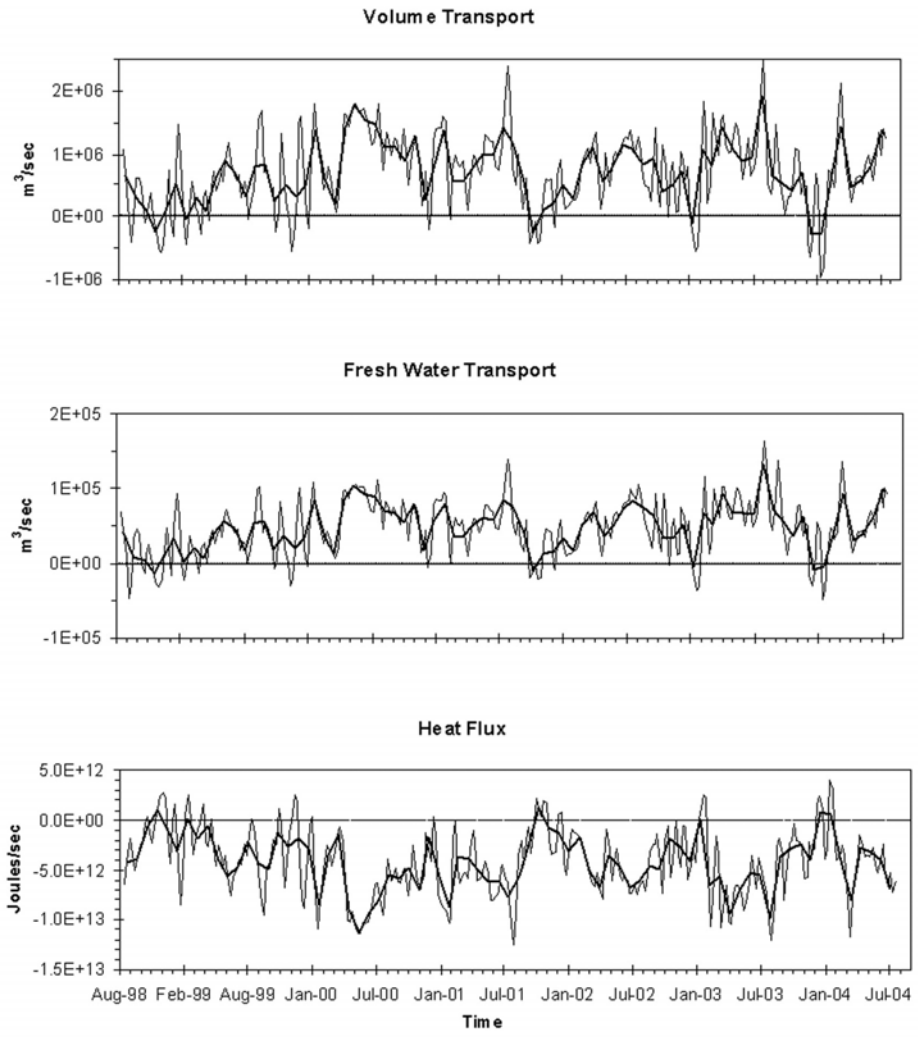

Figure 6. Time series of weekly and monthly averaged fluxes through western Lancaster Sound, August 1998 to 2004.

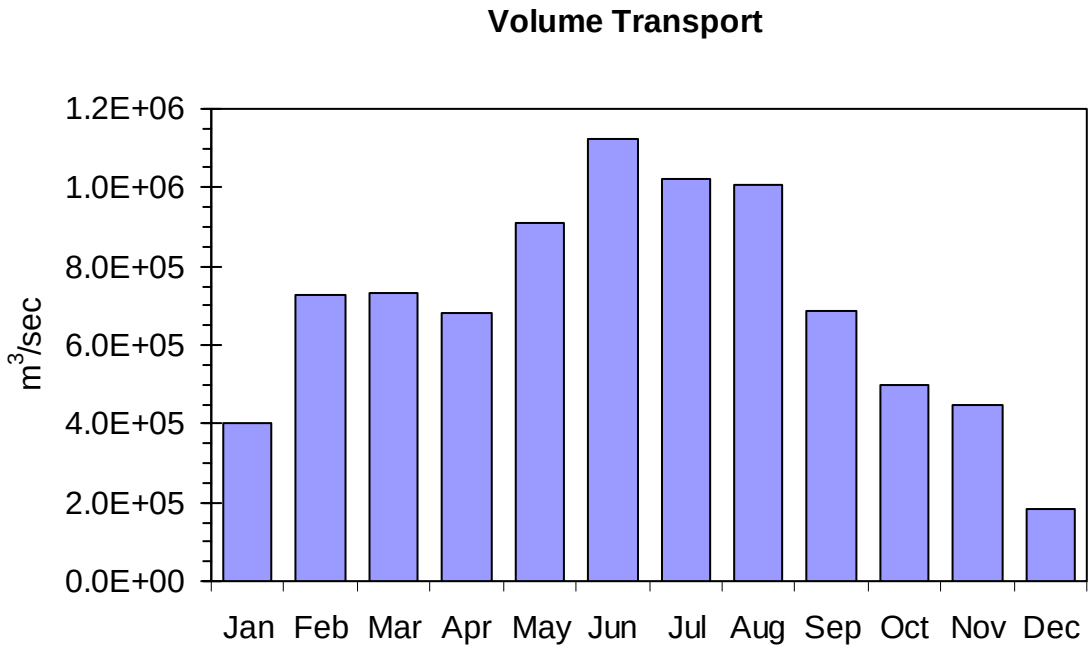

Figure 7. Monthly means of volume flux through western Lancaster Sound, computed for the 6-year period of measurement, August 1998 to 2004.

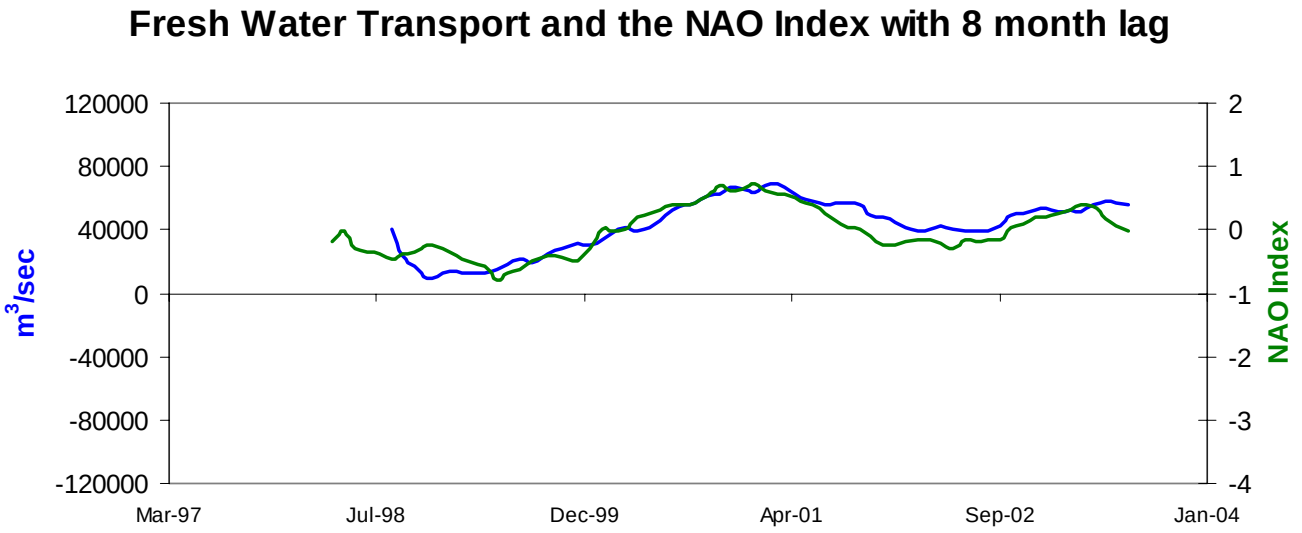

Figure 8. 12-month running averages of fresh-water flux through Lancaster Sound and of the NAO index, with the latter delayed by 8 months.

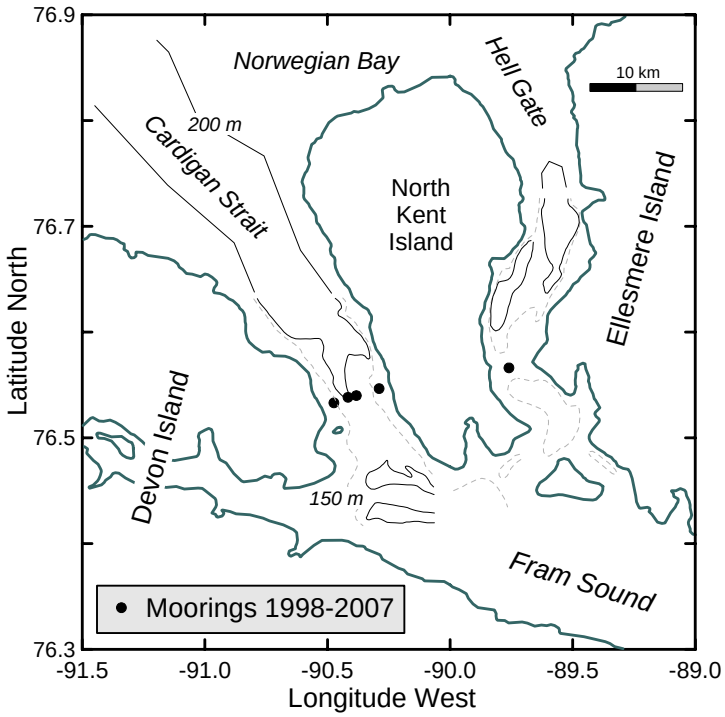

Figure 9. Cardigan Strait and Hell Gate, showing the locations of moorings at the sills. The plotted 150 and 200-m isobaths are based on sparse soundings.

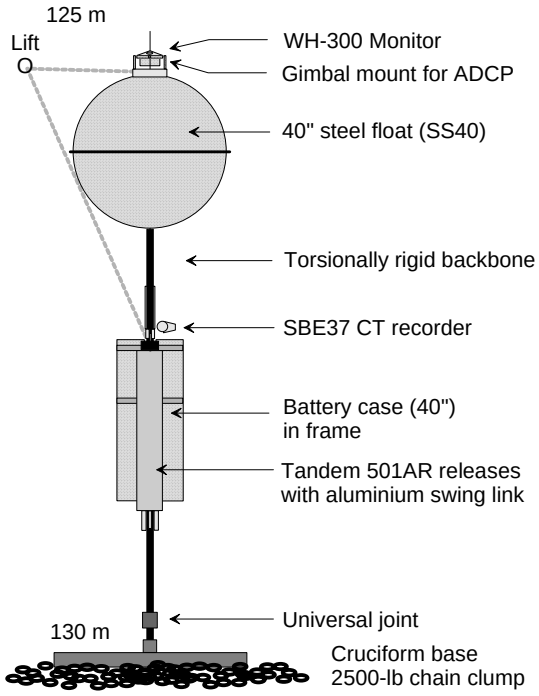

Figure 10. Torsionally rigid mooring designed to address the various difficulties of measuring current in the Canadian Arctic Archipelago.

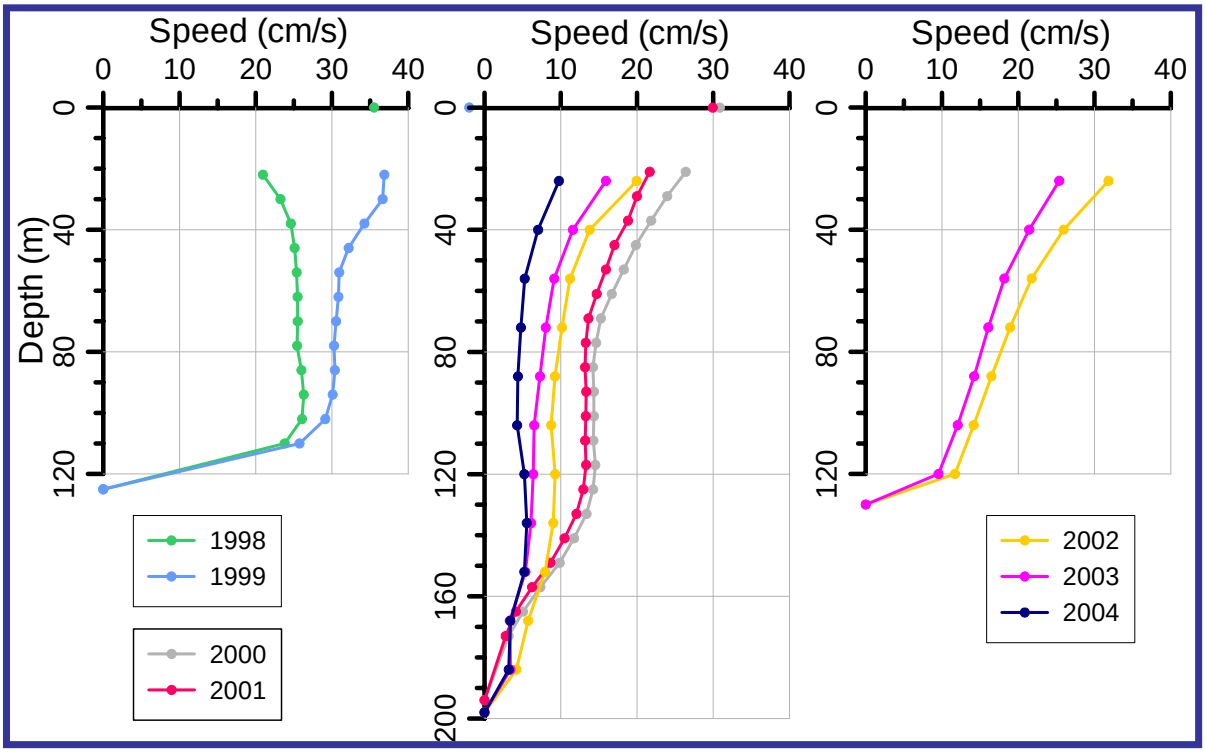

Figure 11. Mean annual profiles of along-channel flow at 3 locations across Cardigan Strait, 1998-2005. An ADCP operated on the western slope during August 1998-2000 (left panel), on the central axis during August 2000-2005 (middle panel) and on the eastern slope during August 2002-2004 (right panel). Labels denote the starting August for the 12-month average. All flows are towards Baffin Bay.

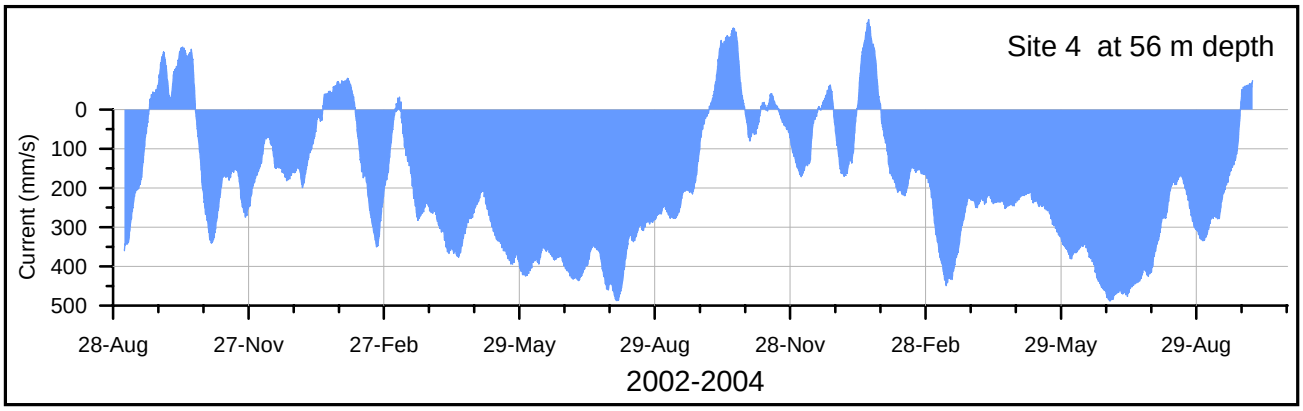

Figure 12. Current at mid depth on the eastern slope of Cardigan Strait, August 2002 to 2004. The record has been filtered to attenuate tides.

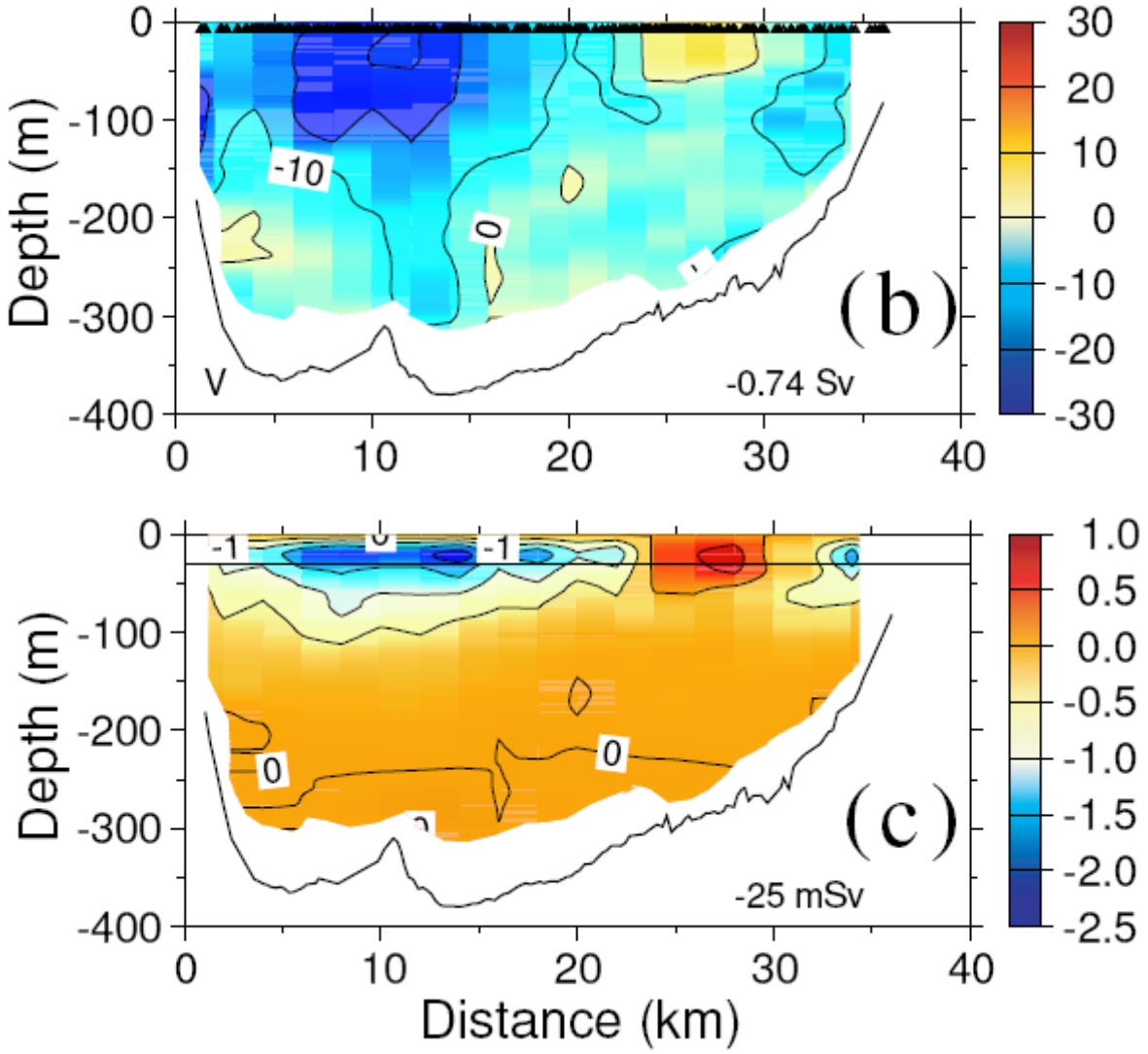

Figure 13. Distribution of volume flux (upper panel) and fresh-water flux (lower panel) through a cross-section near 80.5ºN in Kennedy Channel. Flow out of the Arctic has negative value. Data were collected over a short period in August 2003. The horizontal line near the top of the lower frame marks the depth above which current was estimated, not measured.

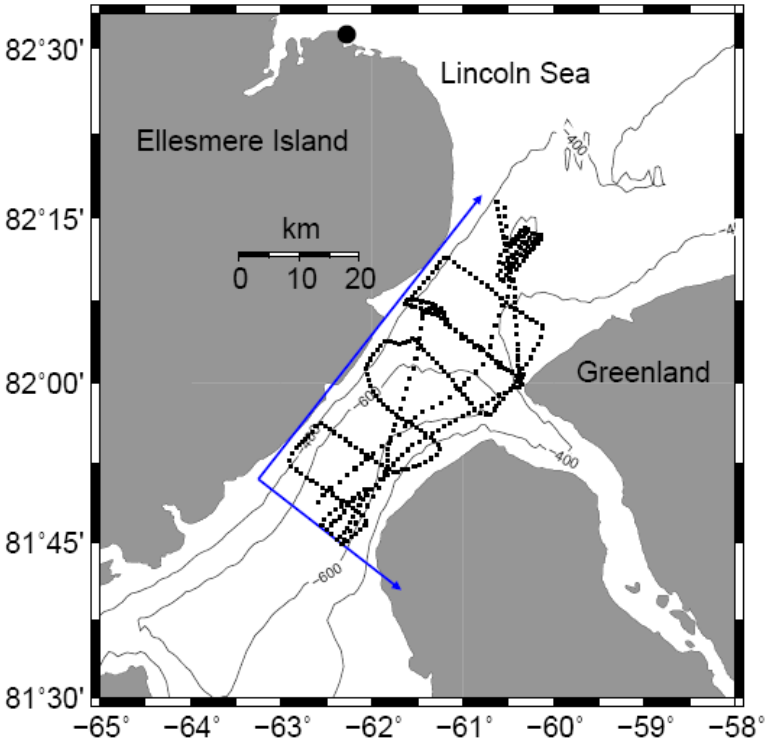

Figure 14. Locations along the track of USCGC Healy where current profiles were measured during 7-11 August 2003.

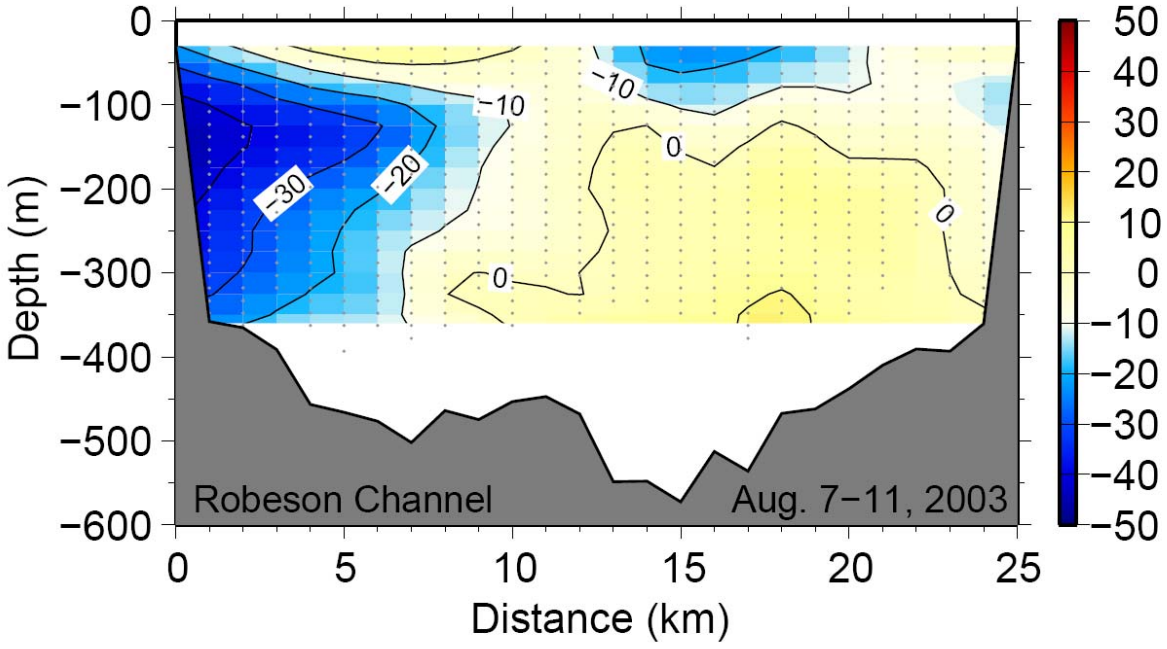

Figure 15. Non-tidal current through Robeson Channel, 7-11 August 2003. Negative values are flow out of the Arctic. The blank area near the top of the frame is too shallow for measurement by the hull-mounted sonar; that below 350 m is beyond the effective operating range of the sonar.

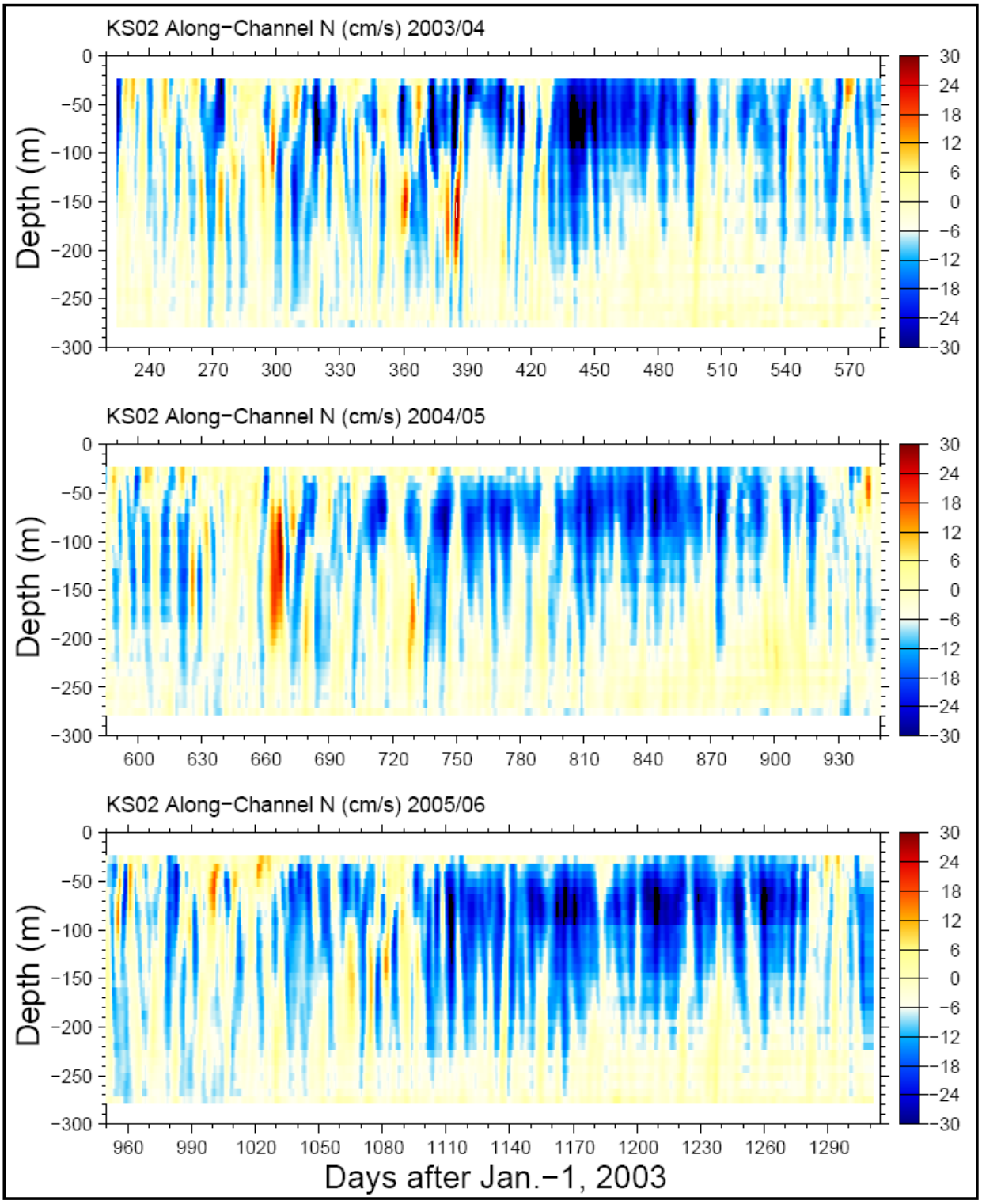

Figure 16. Time series of current along Kennedy Channel near Ellesmere Island from August 2003-2006; tides have been removed. The most obvious variability occurs at periods typical of synoptic weather.

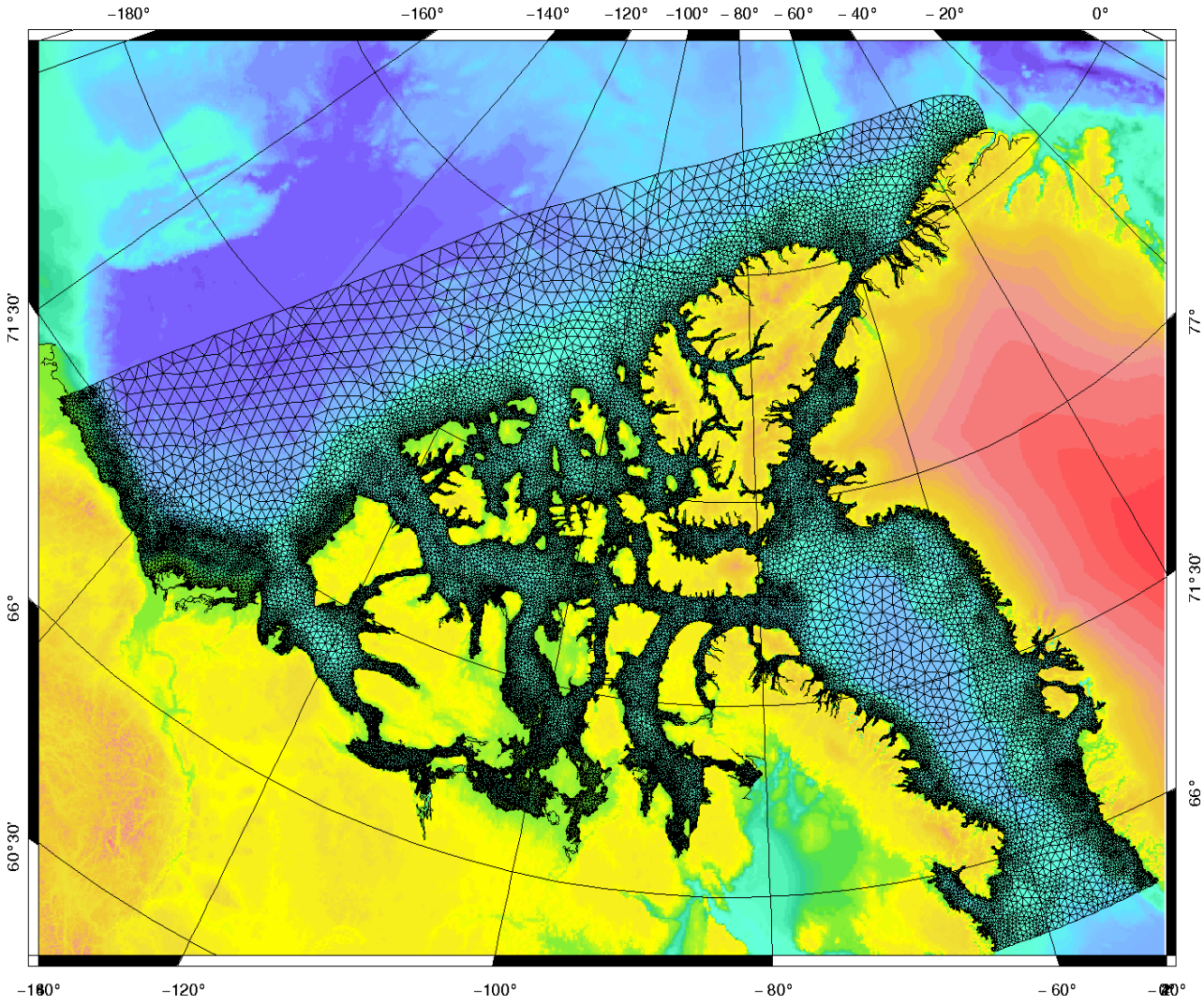

Figure 17. The irregular triangular grid currently used for numerical simulation of circulation over the Canadian polar shelf. There are 76,000 elements (triangles) and 44,000 nodes (computation points). The mean separation of nodes is 7.8 km; the minimum and maximum are 1.1 and 80 km. Kliem and Greenberg (2003) used 20,000 elements and 12,000 nodes with 2.3-83 km separation.

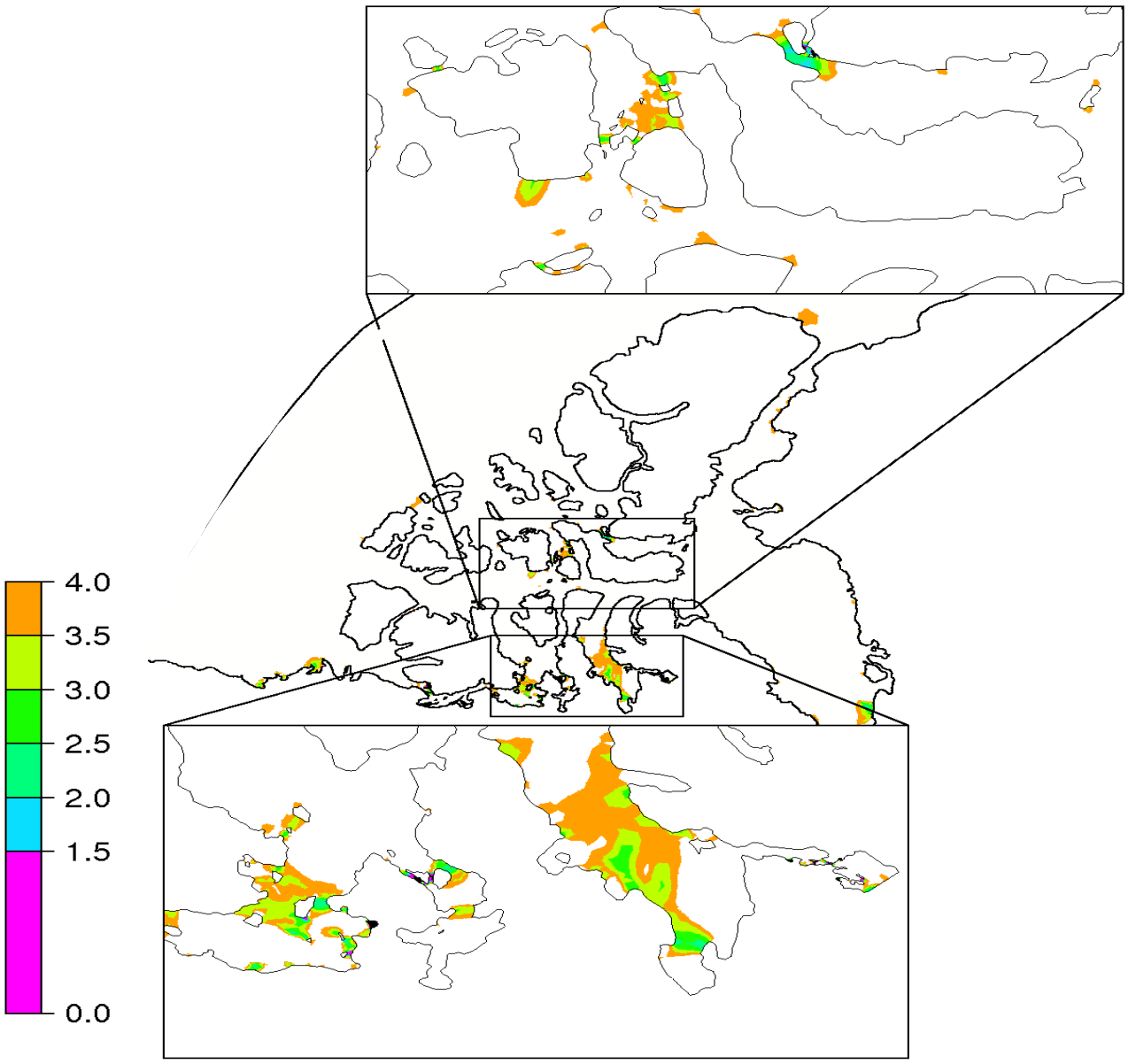

Figure 18. The tidal mixing factor h/u^3 (contours are logarithmically spaced). Two regions with the smallest values (strongest mixing) are expanded for detail. The upper inset is centred on Hell Gate, Cardigan Strait, Queens Channel and Penny Strait. The lower is the region around the Boothia Peninsula. (after Dunphy et al. 2005).

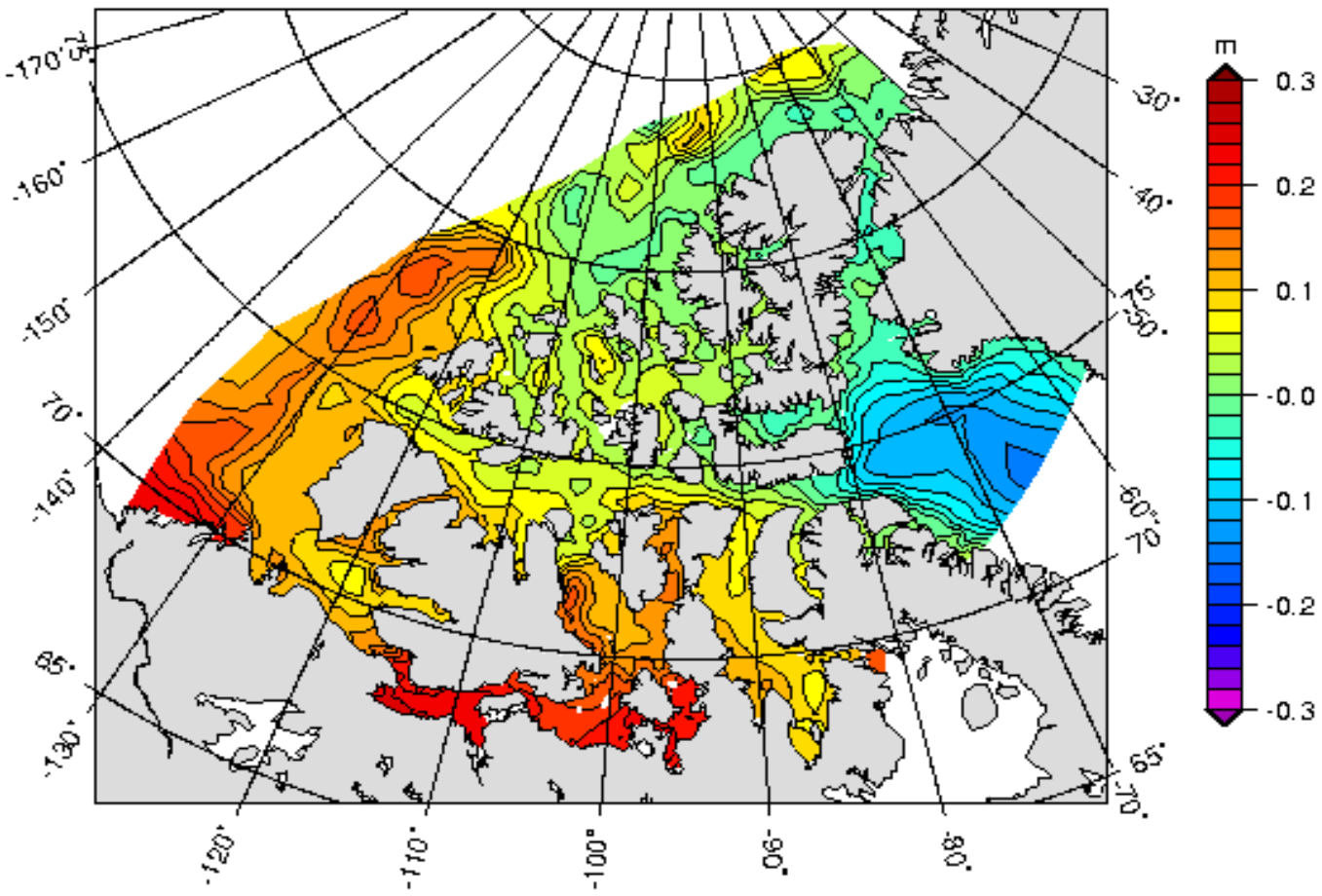

Figure 19. Surface elevation as a proxy for transport (Nicolai Kliem DMI personal communication and http://ocean.dmi.dk/staff/nk/ArcticArchipelago/ - 3D non-linear diagnostic).

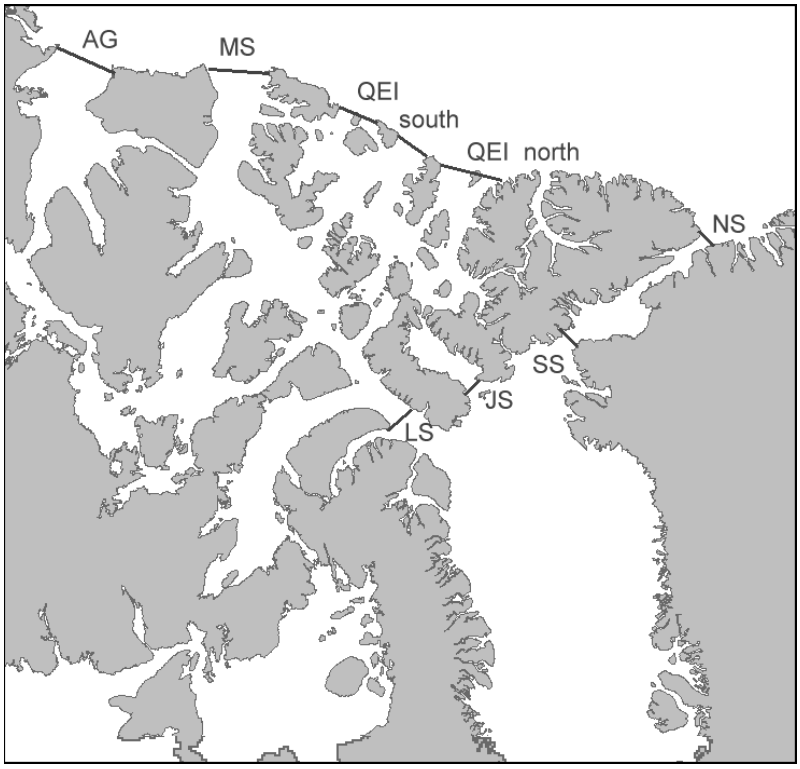

Figure 20. Gateways for calculation of ice-area flux from sequential satellite images.

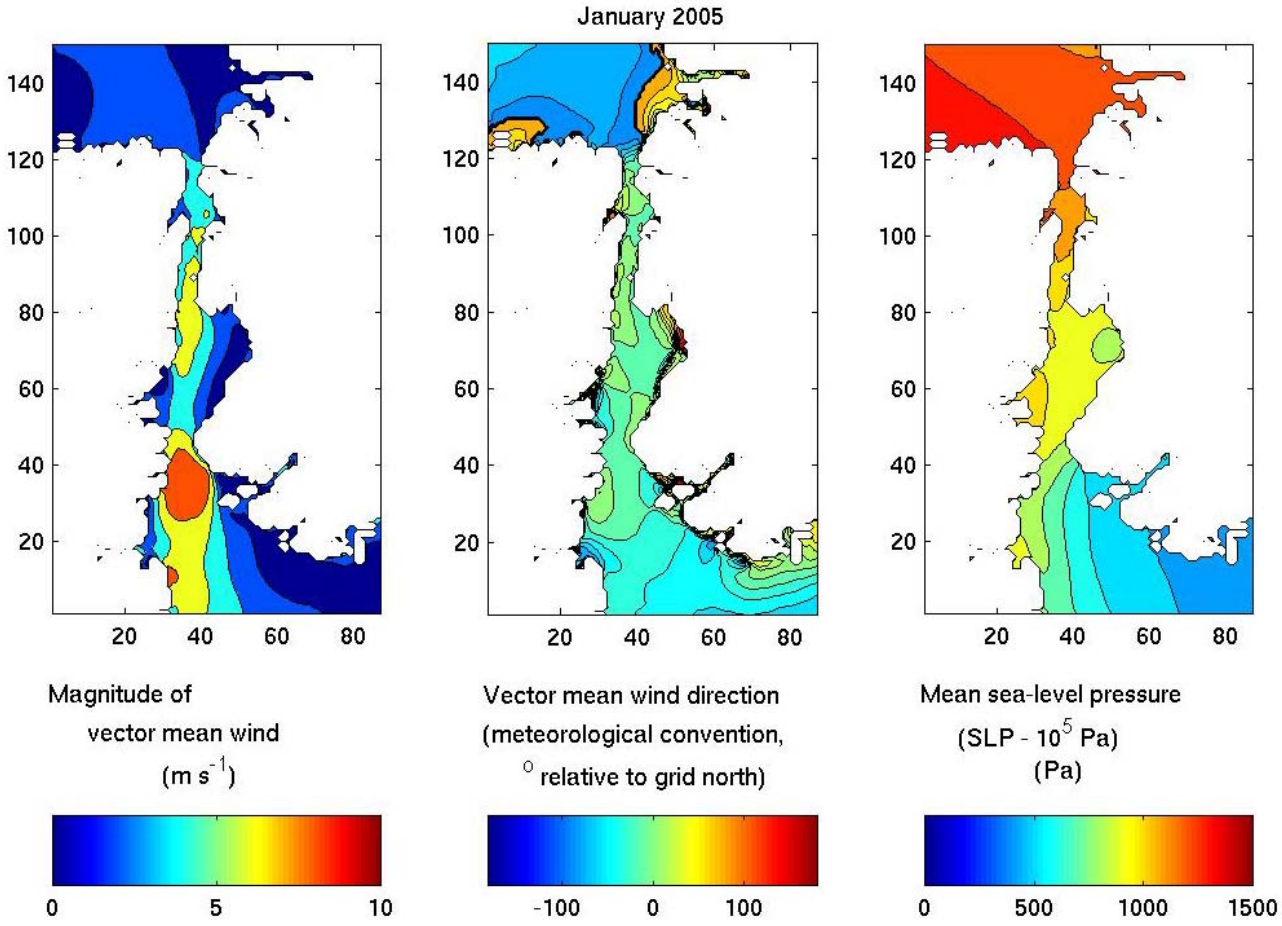

Figure 21. Average fields of sea-level pressure and vector wind for January 2005. These data from simulations using the MM5 clearly reveal meteorological features on both synoptic and meso scales.

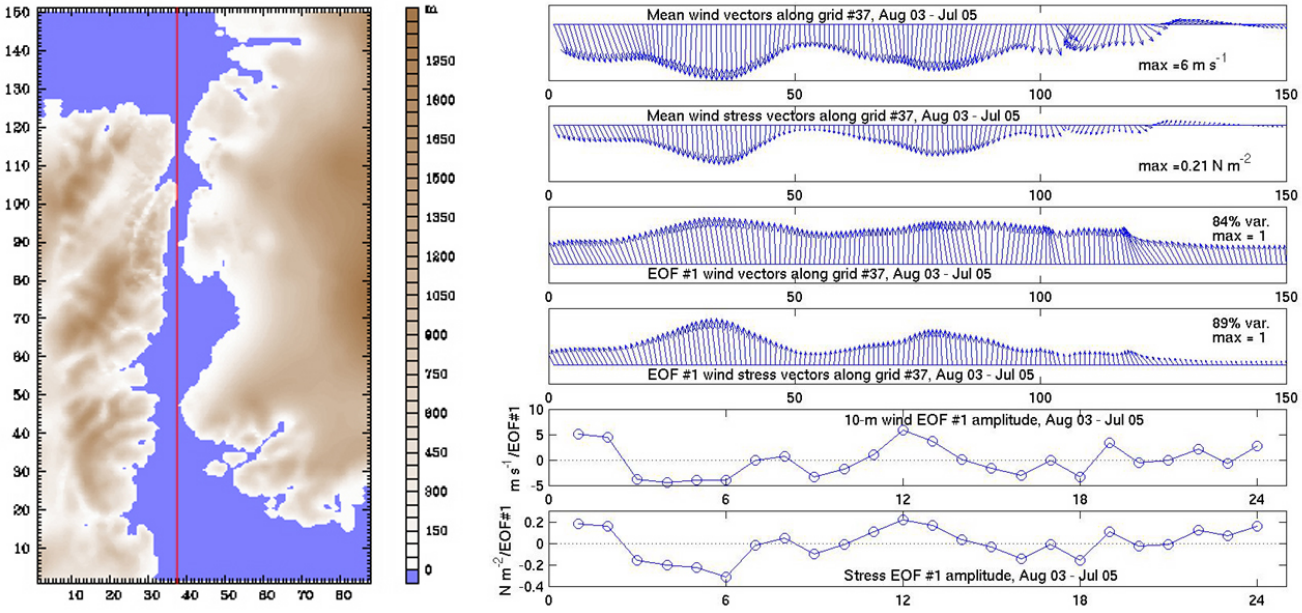

Figure 22. Vectors in the panels on the upper right display the mean wind and stress and the principal EOFs of these variables plotted against grid number along the line marked on the adjacent map; grid number increases from south to north. The panels on the lower right display the eigenvalues plotted against month, beginning in August 2003.

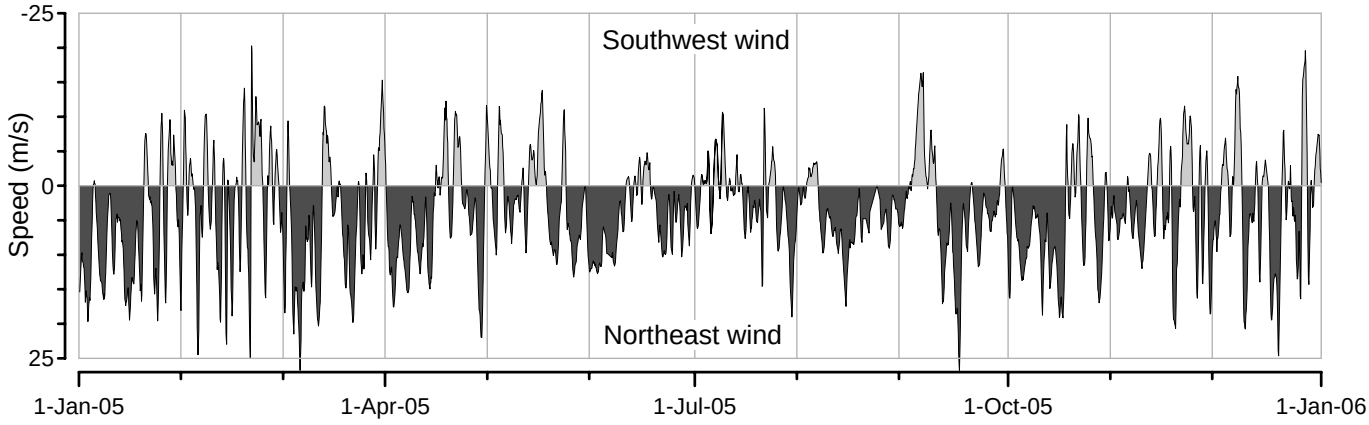

Figure 23. Year-long series of along-channel surface wind in Nares Strait, calculated using the linear dependence of wind on the along-channel difference in sea-level pressure established by Samelson et al. (2006). Pressure was measured at Alert and on the Carey Islands.

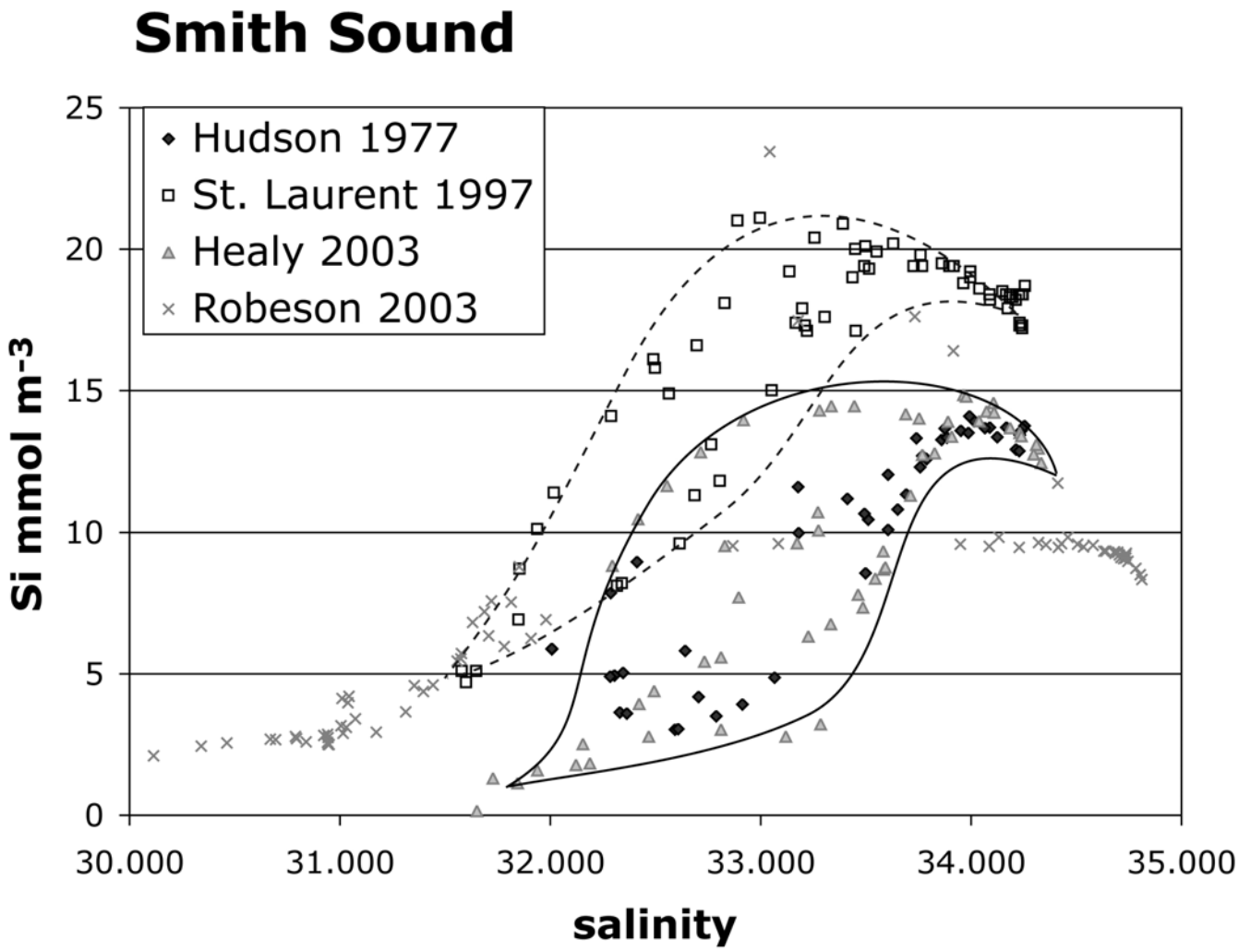

Figure 24. Silicate versus salinity for seawater samples acquired in Smith Sound during August of several years. Added curves envelope data from 1977 and 2003 (solid lines) and from 1997 (dashed line). Within both envelopes, the concentration is highest on the western side of the straits, although in 1977 ice prevented sampling on the western side. Note the shift to more concentrated silica in 1997. Note also the high silica concentration (strong Pacific influence) in northern Nares Strait in 2003; these values from Robeson Channel are comparable to those measured 600 km to the south in Smith Sound in 1997 (Falkner et al., 2006).

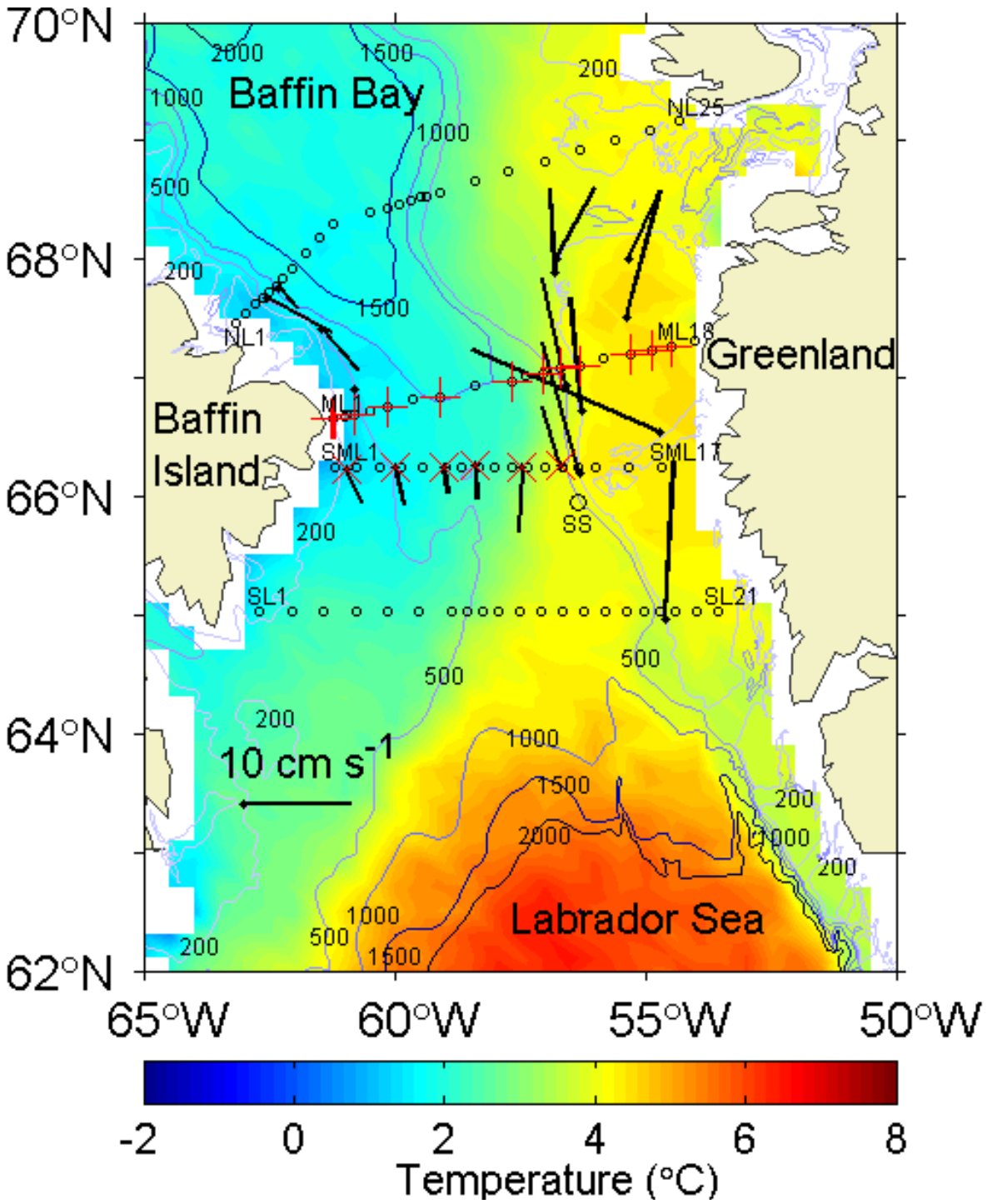

Figure 25. Bathymetry of Davis Strait. The coloured underlay represents long-term mean sea-surface temperature. Square symbols mark the locations of moorings placed in September 2004 in a new initiative to measure oceanic fluxes. Open circles mark recent conventional hydrographic surveys. Vectors depict depth-averaged current from instruments on moorings in the 1980s.

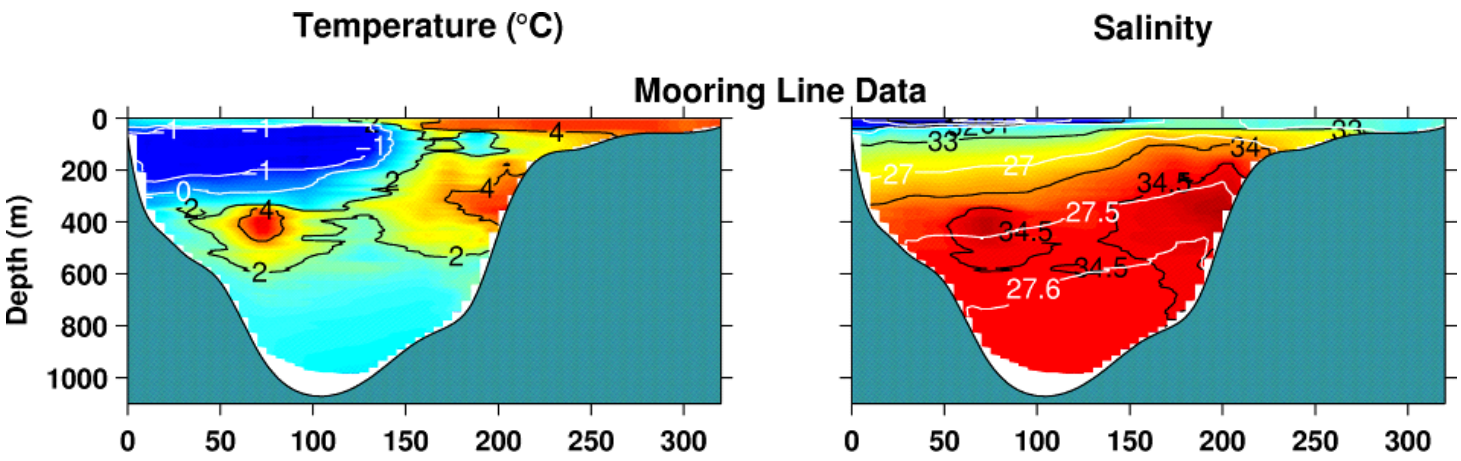

Figure 26. Hydrographic section across Davis Strait measured in September 2004, showing temperature (ºC, left panel) and salinity (right panel). The station spacing was about 25 km.

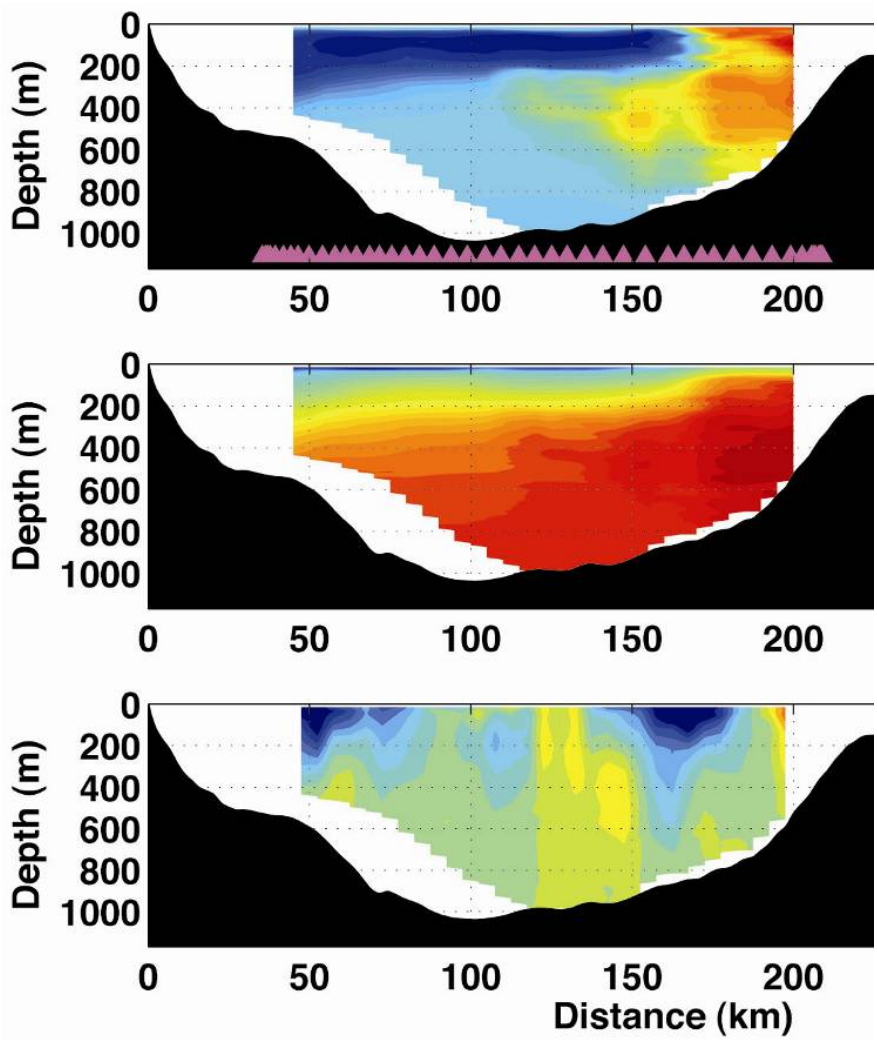

Figure 27. Hydrographic structure within the deep trough of Davis Strait measured by Sea Glider at approximately 5-km resolution.

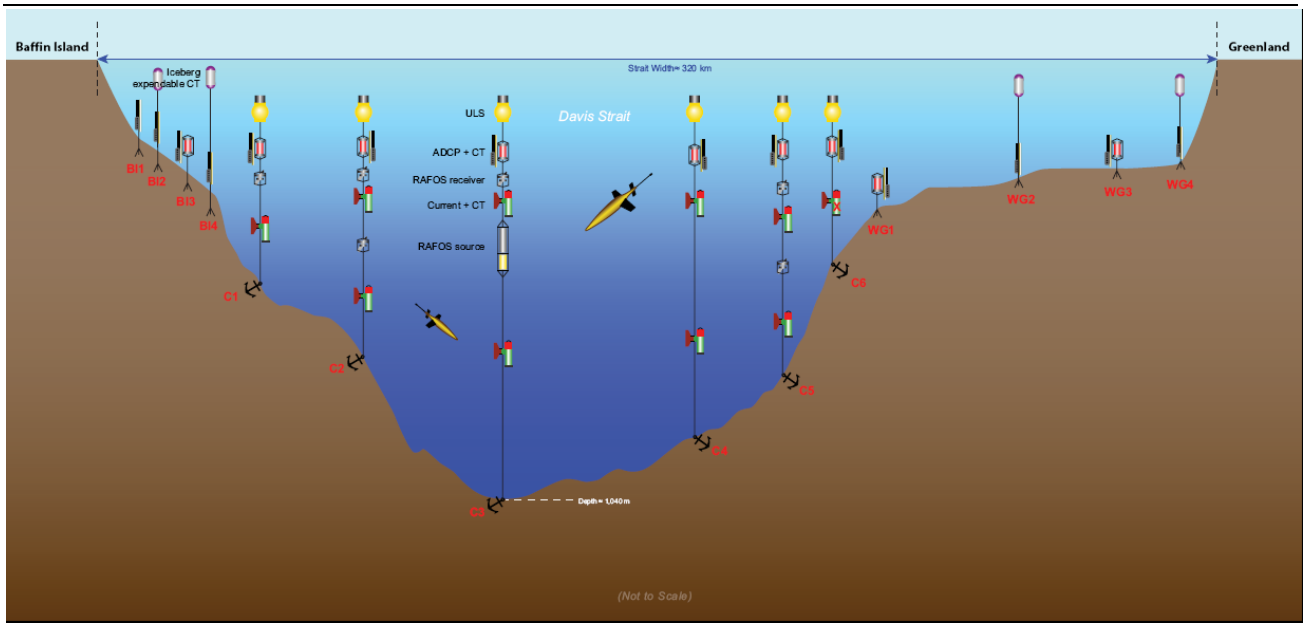

Figure 28. Schematic representation of the array of instruments to measure fresh-water flux through Davis Strait.

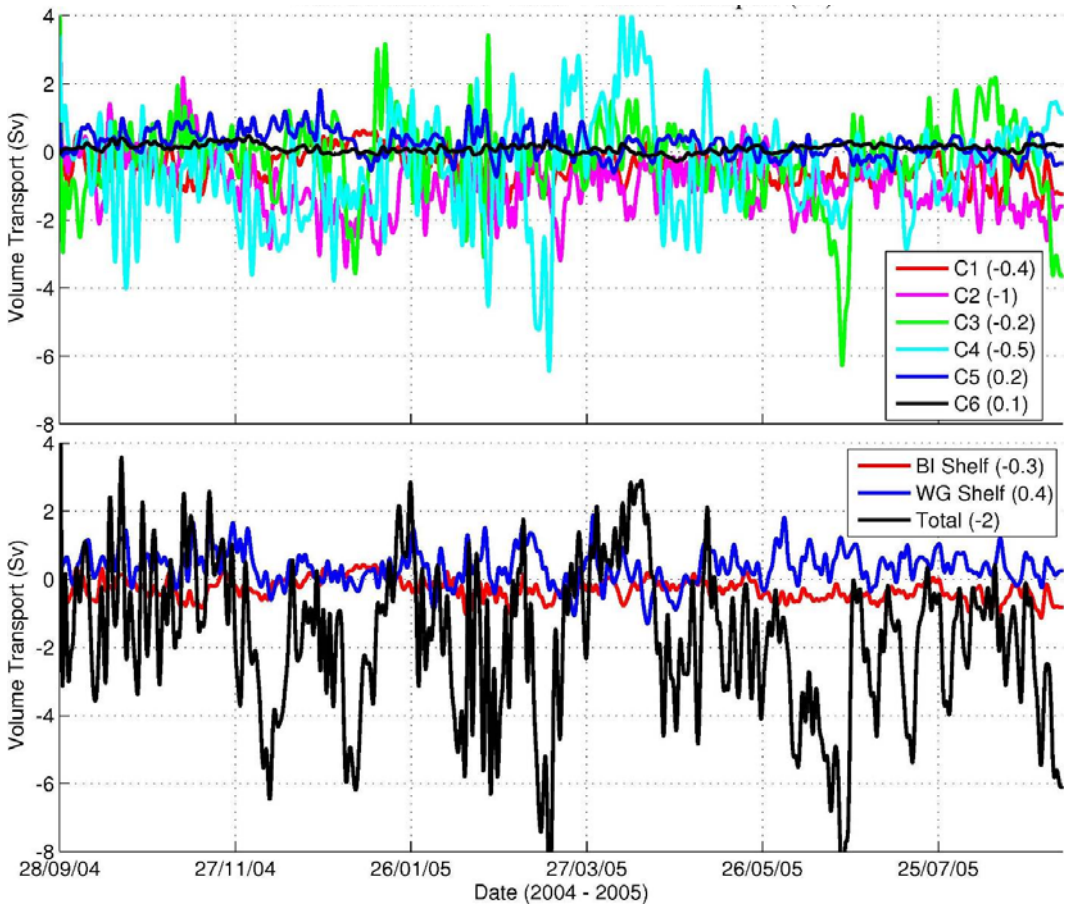

Figure 29. Time series of area-weighted contributions to volume flux through Davis Strait, based on data from individual moorings during September 2004-2005.

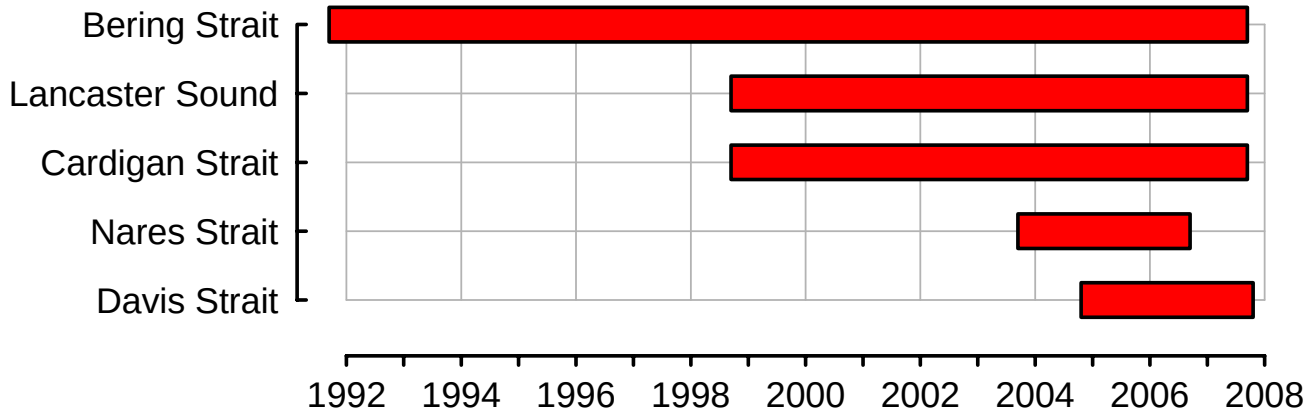

Figure 30. Lifetimes of moored arrays within the gateways for Pacific-Arctic through-flow. The bars span those years during which current was measured for much of the time, but perhaps not in sufficient detail to permit the calculation of fluxes.